T.C.
REPUBLIC OF TURKEY
HACETTEPE UNIVERSITY
GRADUATE SCHOOL OF HEALTH SCIENCES

TO EXAMINE THE ROLE OF HYPOXIA ON ANTI-TUMOUR IMMUNITY

Rüveyda AYASUN, MD

Tumor Biology and Immunology Program

DOCTOR OF PHILOSOPHY THESIS

ANKARA

2021

T.C.
REPUBLIC OF TURKEY
HACETTEPE UNIVERSITY
GRADUATE SCHOOL OF HEALTH SCIENCES

TO EXAMINE THE ROLE OF HYPOXIA ON ANTI-TUMOUR IMMUNITY

Rüveyda AYASUN, MD

Tumor Biology and Immunology Program

DOCTOR OF PHILOSOPHY THESIS

ADVISOR

Assoc. Prof. Füsun Özmen

CO-ADVISOR

Prof. Susan Kaech

ANKARA

2021

ONAY SAYFASI

HACETTEPE UNIVERSITY

GRADUATE SCHOOL OF HEALTH SCIENCES

TO EXAMINE THE ROLE OF HYPOXIA ON ANTI-TUMOUR IMMUNITY

Rüveyda Ayasun

Supervisor: Assoc. Prof. Füsun Özmen

Co-supervisor: Prof. Susan Kaech

This thesis study has been approved and accepted as a PhD dissertation in "Tumor Biology and Immunology Program" " by the assesment committee, whose members are listed below, on 05.03.2021

Chairman of the Committee :	***Prof. A. Lale Doğan*** *Hacettepe University*
Member :	***Prof. Ayşegül Atak Yücel*** *Gazi University*
Member :	***Prof. İbrahim H. Güllü*** *Hacettepe University*
Member :	***Prof. Hakan Akbulut*** Ankara University
Member :	***Asst. Prof. Begüm Kocatürk*** *Hacettepe University*

This dissertation has been approved by the above committee in conformity to the related issues of Hacettepe University Graduate Education and Examination Regulation.

26 Mayıs 2021

Prof. Diclehan ORHAN, MD, PhD

Director

YAYIMLAMA VE FİKRİ MÜLKİYET HAKLARI BEYANI

Enstitü tarafından onaylanan lisansüstü tezimin/raporumun tamamını veya herhangi bir kısmını, basılı (kağıt) ve elektronik formatta arşivleme ve aşağıda verilen koşullarla kullanıma açma iznini Hacettepe Üniversitesine verdiğimi bildiririm. Bu izinle Üniversiteye verilen kullanım hakları dışındaki tüm fikri mülkiyet haklarım bende kalacak, tezimin tamamının ya da bir bölümünün gelecekteki çalışmalarda (makale, kitap, lisans ve patent vb.) kullanım hakları bana ait olacaktır.

Tezin kendi orijinal çalışmam olduğunu, başkalarının haklarını ihlal etmediğimi ve tezimin tek yetkili sahibi olduğumu beyan ve taahhüt ederim. Tezimde yer alan telif hakkı bulunan ve sahiplerinden yazılı izin alınarak kullanılması zorunlu metinlerin yazılı izin alınarak kullandığımı ve istenildiğinde suretlerini Üniversiteye teslim etmeyi taahhüt ederim.

Yükseköğretim Kurulu tarafından yayınlanan ***"Lisansüstü Tezlerin Elektronik Ortamda Toplanması, Düzenlenmesi ve Erişime Açılmasına İlişkin Yönerge"*** kapsamında tezim aşağıda belirtilen koşullar haricince YÖK Ulusal Tez Merkezi / H.Ü. Kütüphaneleri Açık Erişim Sisteminde erişime açılır.

- ○ Enstitü / Fakülte yönetim kurulu kararı ile tezimin erişime açılması mezuniyet tarihimden itibaren 2 yıl ertelenmiştir. (1)
- **X** Enstitü / Fakülte yönetim kurulunun gerekçeli kararı ile tezimin erişime açılması mezuniyet tarihimden itibaren 6 ay ertelenmiştir. (2)
- ○ Tezimle ilgili gizlilik kararı verilmiştir. (3)

03/05/2021

Dr. Rüveyda AYASUN

[i] *"Lisansüstü Tezlerin Elektronik Ortamda Toplanması, Düzenlenmesi ve Erişime Açılmasına İlişkin Yönerge"*

*(1) Madde 6. 1. Lisansüstü tezle ilgili patent başvurusu yapılması veya patent alma sürecinin devam etmesi durumunda, tez **danışmanının** önerisi ve **enstitü anabilim dalının** uygun görüşü üzerine **enstitü** veya **fakülte yönetim kurulu** iki yıl süre ile tezin erişime açılmasının ertelenmesine karar verebilir.*

*(2) Madde 6. 2. Yeni teknik, materyal ve metotların kullanıldığı, henüz makaleye dönüşmemiş veya patent gibi yöntemlerle korunmamış ve internetten paylaşılması durumunda 3. şahıslara veya kurumlara haksız kazanç imkanı oluşturabilecek bilgi ve bulguları içeren tezler hakkında tez **danışmanının** önerisi ve **enstitü anabilim dalının** uygun görüşü üzerine **enstitü** veya **fakülte yönetim kurulunun** gerekçeli kararı ile altı ayı aşmamak üzere tezin erişime açılması engellenebilir.*

*(3) Madde 7. 1. Ulusal çıkarları veya güvenliği ilgilendiren, emniyet, istihbarat, savunma ve güvenlik, sağlık vb. konulara ilişkin lisansüstü tezlerle ilgili gizlilik kararı, **tezin yapıldığı kurum** tarafından verilir *. Kurum ve kuruluşlarla yapılan işbirliği protokolü çerçevesinde hazırlanan lisansüstü tezlere ilişkin gizlilik kararı ise, **ilgili kurum ve kuruluşun önerisi** ile **enstitü** veya **fakültenin** uygun görüşü üzerine **üniversite yönetim kurulu** tarafından verilir. Gizlilik kararı verilen tezler Yükseköğretim Kuruluna bildirilir.*
Madde 7.2. Gizlilik kararı verilen tezler gizlilik süresince enstitü veya fakülte tarafından gizlilik kuralları çerçevesinde muhafaza edilir, gizlilik kararının kaldırılması halinde Tez Otomasyon Sistemine yüklenir

** Tez danışmanının önerisi ve enstitü anabilim dalının uygun görüşü üzerine enstitü veya fakülte yönetim kurulu tarafından karar verilir.*

ETHICAL DECLARATION

In this thesis study, I declare that all the information and documents have been obtained in the base of the academic rules and all audio-visual and written information and results have been presented according to the rules of scientific ethics. I did not do any distortion in data set. In case of using other works, related studies have been fully cited in accordance with the scientific standards. I also declare that my thesis study is original except cited references. It was produced by myself in consultation with advisor and co-advisor (Assoc.Prof. Füsun Özmen and Prof. Dr. Susan Kaech, respectively) and written according to the rules of thesis writing of Hacettepe University Institute of Health Sciences.

Rüveyda AYASUN, MD

ACKNOWLEDGEMENTS

First and foremost, I would like to thank my mentors Dr. Füsun Özmen and Dr. Susan Kaech for their guidance and support during my graduate studies. I feel extremely lucky to have worked with these two great mentors whom had a great impact on my scientific approach and academic career. Both of my mentors' enthusiasm to scientific discovery always fascinated me.

I also feel very lucky to be a part of the MD/PhD program and Basic Oncology Department at Hacettepe University. I would like to thank my thesis dissertation committee Dr. A. Lale Doğan and Dr. Hakan Akbulut for their invaluable support throughout my graduate education. The financial support from the TÜBİTAK 2214/A, Vehbi Koc Foundation, YÖK 100/2000, and Melanoma Research Alliance has also been very helpful during my graduate work.

My story in the Kaech Lab started at Yale School of Medicine where I worked most closely with Dr. Fabio Santori. His limitless support helped me immensely in developing my laboratory skills. I would also like to specially thank Drs. Victor Du, Dan Chen and Tom Mann for being great friends both in and outside of the lab.

I feel very lucky to have had the support of my aunt, Hülya Ayasun-Genovese. Her tremendous effort to help me thrive in challenging circumstances was invaluable. Gürol Akman and Mahide Akman truly treated me like a daughter. Indeed, I already miss their sincerity.

Last, but certainly not least, I would like to thank my family for their unceasing support and encouragement. I thank my mom, Semra Ayasun, for being a true inspiration for me. With her hardworking and strong personality, she has always been a role-model for me. I thank my dad, Mustafa Ayasun, who was always there to help me achieve my goals. His caring personality helped me to discover my full potential. I cannot thank enough my sisters, Ilayda and Bilge Safiye, for their patience and support during both good and challenging times. I thank my grandma, Meliha Ayasun, for always being with me during my journey. I would not be where I am today without her support during my education. I would like to dedicate this thesis and all my accomplishments to my dear family.

ABSTRACT

Ayasun, R., To examine the role of hypoxia on anti-tumour immunity, Hacettepe University Graduate School of Health Sciences, Tumor Biology and Immunology Program, Doctor of Philosophy Thesis, Ankara, 2021. Inhibition of tumor angiogenesis has been extensively utilized in the treatment of metastatic colorectal cancer and renal cell carcinoma. Complete disruption of tumor angiogenesis results in hypoxia which promotes tumor metastasis and treatment resistance. Although angiogenesis inhibitors are successful to some extent, majority of patients experience the recurrence and acquired resistance. Spatial and temporal changes in tumor microenvironment sculpt the anti-tumor immune response. However, little is known how tumor oxygenation and vessel normalization *in vivo* influence immune infiltration in YUMMER melanoma tumors. We hypothesized that tumor vessel structure implicates in immune cell composition in melanoma. Therefore, we utilized a previously well-defined mouse model which targets one copy of *Phd2* gene. Haplodeficiency of *Phd2* normalizes the endothelial alignment and improves pericyte coverage of blood vessels, thereby increasing tumor perfusion and oxygenation. We demonstrated that mitigation of "true" hypoxia through blood vessel normalization improves anti-tumor immunity, thereby delaying tumor growth. In addition, our study highlighted that disruption of hypoxia using *Phd2* haplodeficient mouse model re-shaped tumor microenvironment through improved CD4+ and CD8+ T cell infiltration, recruitment of pro-inflammatory macrophages, and diminished infiltration of PD-L1^{hi} anti-inflammatory macrophages. Subsequently, tumor growth is delayed in a T cell dependent manner. In conclusion, *Phd2* haplodeficiency restores tumor oxygenation and enhances anti-tumor immune cell infiltration in melanoma tumors.

Key Words: hypoxia, Phd2, vessel normalization, melanoma, anti-tumour immune response

ÖZET

Ayasun, R., Hipoksinin anti-tümör immün yanıt üzerine etkisinin araştırılması, Hacettepe Üniversitesi Sağlık Bilimleri Enstitüsü Tümör Biyolojisi ve İmmünolojisi Programı, Doktora Tezi, Ankara, 2021. Anjiojenez inhibitörleri metastatik kolorektal kanser ve renal hücreli karsinoma tedavisinde çok önemli bir yer edinmektedir. Fakat tümör anjiojenezinin tamamen ortadan kaldırılması ile tümör hipoksisi oluşmaktadır. Solid tümörlerde hipoksinin uzak metastazda ve anti-kanser tedavilere dirençte önemli bir rol aldığı bilinmektedir. Buna istinaden anjiojenez inhibitörü kullanan pek çok kanser hastasında da anjijenez inhibitörlerinin etkinliği kısıtlı kalmakta olup tedaviye karşı kazanılmış direnç ve hastalık rekürrensi en sık karşılaşılan problemlerden biridir. Tümör mikroçevresindeki lokalize ve zamansal değişimler anti-tümör immün yanıtları şekillendirmektedir. Buna rağmen in vivo tümör oksijenizasyonunun ve damar normalizasyonunun melanomaya karşı immün yanıtı nasıl etkilediği tam olarak anlaşılamamıştır. Çalışmaya damar yapısının YUMMER melanoma modelinde immün kompozisyonu etkilediği hipotezi ile başladık. Bunu gösterebilmek için Phd2 haplodefektli fareleri kullandık. Bu defekt sayesinde damarlardaki perisit hücre ile çevrili olma oranı artmış ve endotel hücre dizilimi normalize olmuştur. Sonuç olarak oksijenizasyon artmıştır. Artan oksijenizasyonu takiben CD4+ ve CD8+ T hücre infiltrasyonu ve pro-inflamatuar makrofaj infiltrasyonunun arttığı görülmüştür. Bunun yanında yüksek oranda PD-L1 eksprese eden anti-inflamatuar makrofaj infiltrasyonu da azalmıştır. Bu bulgularla paralel olarak tümör büyümesi T hücre bağımlı bir mekanizma ile yavaşlamıştır. Sonuç olarak fare melanoma modelinde Phd2 haplodefekti tümör oksijenizasyonunu restore etmekte ve anti-tümör immün infiltrasyonu iyileştirmektedir.

Anahtar kelimeler: hipoksi, Phd2, damar normalizasyonu, melanoma, anti-tümör immün yanıtlar

TABLE OF CONTENTS

LIST OF ABBREVIATIONS

α-SMA	Alpha smooth muscle actin
Ab	Antibody
Ag	Antigen
APC	Antigen presenting cells
BFA	Brefeldin A
BOLD	Blood oxygen level-dependent imaging
BSA	Bovine serum albumin
Ca	Calcium
CD	Cluster of differentiation
CSF	Colony stimulating factor
CTL	Cytotoxic T lymphocyte
CTRL	Control
DC	Dendritic cell
ddH_2O	Double distilled water
DMEM	Dulbecco's Modified Eagle's Medium
DMSO	Dimethyl sulfide
DNA	Deoxyribonucleic acid
EDTA	Ethylene diamine tetracetic acid
ELISA	Enzyme-linked immunosorbent assay
FACS	Fluoresecence activated cell sorting
FBS	Fetal bovine serum
FDA	Food and Drug Administration
FDG	18-Fluoro-deoxy-glucose
FIH1	Factor inhibiting HIF1
FITC	Fluorescein isothiocyanate
HIF-1α	Hypoxia inducible factor
HLA	Human leukocyte antigen
HMGB1	High mobility group box protein 1
IFN	Interferon

IFP	Interstitial fluid pressure
IL	Interleukin
i.m	Intramuscular
i.p.	Intraperitoneal
i.v.	Intravenous
Lag3	Lymphocyte activation gene
LCMV	Lymphocytic choriomeningitis virus
LLC	Lewis lung cancer
LN	Lymph node
LPS	Lipopolysaccharide
mAb	Monoclonal antibody
MDSC	Myeloid derived suppressor cells
MHC	Major histocompatibility complex
MMP	Matrix metalloprotease
mRNA	Messenger ribonucleic acid
NF-KB	Nuclear factor kappa B
NO	Nitric oxide
OCT	Optimal Cutting Temperature Compound
PBMC	Peripheral blood mononuclear cells
PBS	Phosphate buffered saline
PD-1	Programmed death-1
PD-L1	Programmed death-ligand 1
PFA	Paraformaldehyde
PHD2	Prolyl hydroxylase-2 Radiation 1.7
RPMI 1640	Roswell Park Memorial Institute 1640
s.c.	Subcutaneous
TAM	Tumor associated macrophage
TCR	T cell receptor
Th	Helper T cell
TIL	Tumor infiltrating lymphocyte

TME	Tumor microenvironment
TNF	Tumor necrosis factor
Treg	Regulatory T cells
VEGF	Vascular endothelial growth factor
VHL	Von Hippel Lindau
WT	Wild type
YUMMER 1.7	Yale University Mouse Melanoma Exposed to Radiation
ZO-1	Zonula occludens-1

LIST OF FIGURES

LIST OF TABLES

1. INTRODUCTION

Malignant proliferation of melanocytes in the epidermis gives rise to melanoma and is a challenging disease as it is capable of metastasizing throughout the body. At early stage of the disease, patients can be treated with chemotherapy following to surgical excision. However, these therapeutic options do not yield survival benefit at later disease course. The lack of effective treatment options urge clinicians to develop new therapeutics. Recently, it has been highlighted that immune check point inhibitors provide a survival benefit to patients with non-small cell lung cancer (NSCLC), bladder cancer, and melanoma to some extent. Overall survival metastatic melanoma patients was 6 to 9 months under traditional treatments. Targeted therapies such as vemurafenib (B-raf inhibitor) as well as chemotherapy agents have shown promising results, however, survival benefits are far from clinical significance (1). Nevertheless, T cell based-immune check point inhibitors (ICIs) are now approved by Food and Drug Administration (FDA) and are used first line treatment for several cancers consisting of melanoma, renal cell carcinoma etc. Recently, some patients with melanoma exhibit remarkable responses to ICIs (2) regardless of its highly metastatic aspect. However, one of the major obstacles clinicians face with is that not every patient responds immunotherapy, instead majority of patients develop resistance over the course of treatment (3). In addition to acquired resistance, some of the patients must discontinue immunotherapy due to life-threatening adverse effects. Therefore, novel approaches are warranted for patients who are not responsive to ICIs.

It is now appreciated that cancer cells co-exist in a chaotic environment with neighboring stromal and immune cells. Moreover, cancer cells' interactions with components of the tumor microenvironment (TME) impact their growth and metastasis (4). In this complexity, when tumors reach a certain size, they incite new blood vessel formation which is termed as angiogenesis in order to cope with their increased oxygen and nutrient demand. Angiogenetic tumor vessels are disorganized and fragile by virtue of aberrations in their endothelial lining (i.e, misalignment) and pericyte coverage (5). Losing of hierarchical architecture; and an abnormal

endothelial alignment contributes to the pro-carcinogenic and immunosuppressive TME. This dysregulation maintains a cancer cell's permissive environment characterized by hypoxia. Subsequently, this chaotic environment generates a physical barrier to T cell infiltration (4). Recent studies have demonstrated that blood endothelial cells as well as lymphatic endothelial cells within TME can effectively suppress recruitment, adhesion, extravasation, and functionality of T cells (6, 7). Besides, macrophages are prominent cell types within most tumors and their differentiation into pro-inflammatory macrophages may be hampered by oxygen shortage (8). Moreover, some studies have highlighted the implication of hypoxia in upregulating PD-L1 expression on myeloid derived suppressor cells (MDSC) (9). It has been demonstrated previously that PD-L1^{hi} F4/80^{hi} macrophages show anti-inflammatory features. In contrast, TNFα-producing macrophages are F4/80^{int} Ki67^{+} suggesting that they are M1 like proinflammatory macrophages (10).

2.GENERAL INFORMATION

2.1. Melanoma

Melanoma arises from the melanocytes in the epidermis and accounts for 5% of patients who are diagnosed with cancer each year. Even though it has a favorable outcome when diagnosed early in the disease course, melanoma has a dismal prognosis with 25% of survival rate in patients with advanced metastatic disease (11). Historically, melanoma patients underwent surgical excision, if resectable, followed by chemotherapy. However, toxicities-associated with cytotoxic treatments sometimes outweigh the clinical benefit. Therefore, in an era of precision medicine, novel treatment options (e.g. targeted therapy, immunotherapy) are emerging to improve outcome in patients with advanced metastatic melanoma. Recently, next-generation-sequencing (NGS) has revolutionized the cancer treatment by enabling the identification of actionable targets implicated in disease progression (12). For instance, melanoma patients whose tumors harboring BRAF V600E mutation exclusively responded to BRAF inhibitors (eg, vemurafenib and dafrafenib) with the response rates of more than 50% (13, 14). Nonetheless, patients who were administered small molecule inhibitors eventually became resistant to given medications due to compensatory mechanisms (15). Although further investigations regarding resistance to BRAF inhibitors are underway, cancer researchers have zeroed in targeting neighboring cells within TME instead of genetically unstable and adaptable cancer cells. More recently, exploiting the patient's own immune system against cancer has been recognized as a 5^{th} pillar of cancer treatment along with radiotherapy, chemotherapy, targeted therapy, and surgery. Moreover, FDA has approved several immunotherapy agents as first-line treatment for various cancer types which have been attributed as hard-to-treat diseases previously. For instance, nivolumab was approved by FDA for the first-line therapy of patients with unresectable or metastatic melanoma with the objective response rates (ORR) of 32% in December 2014 (1, 16).

2.2. Tumor Microenvironment

TME consists of a variety of cell types and nutrients. Cellular components of TME include cancer associated fibroblasts (CAF), lymphocytes, dendritic cells (DC), MDSC, tumor associated macrophages (TAM), and extracellular matrix (ECM). Moreover, components of TME continuously cross-talk with cancer cells as well as each other, in turn proceed tumor progression even metastasis (17). When tumors reach a certain size, cancer cells induce vessel formation which is termed as angiogenesis. Angiogenetic vessels are disorganized and are unable to deliver sufficient nutrient and oxygen within solid tumors. This shortage creates hostile microenvironment for cancer cells and adjacent structures. Even though it seems beneficial for tumor cells, it is contradictory for other cell types residing in tumors such as immune cells. Hypoxia, which refers to oxygen shortage, is a well-known aspect of solid tumors and has been extensively studied thus far. Hypoxia contributes tortuous vessel formation, glucose metabolism, stemness feature of cancer cells, and resistance to radiotherapy as well as chemotherapy. However, majority of studies have done by utilizing in vitro models due to paucity of in vivo model which allows us to manipulate tumor oxygenation. Recently, researchers uncovered that supplementary oxygenation decreases tumor metastasis and facilitates influx of CD4+ and CD8+ T cells in given tumor models. For instance, how “true hypoxia” shapes microenvironment. In some studies, researchers have demonstrated that evofosfamide which disrupts hypoxia within tumors may potentiate immune check point blockade efficacy. However, evofosfamide is not specific to target hypoxia but also a chemotherapeutic drug which mediates unspecific cell death. Besides its potential beneficial effect on anti-tumor response, there are controversial studies wherein researchers showed that in vitro cultured T cells under hypoxic condition efficiently prime within tumors and cause delayed tumor progression.

2.3. Hypoxia

Hypoxia which refers low oxygen tension has been a well-known aspect of solid tumors for decades. Initially, hypoxia has been described in the context of

resistance to radiotherapy (18). In 1904, Hahn and Schwarz were able to demonstrate that diminished blood flow abrogated the influences of low energy X-rays. Furthermore, Crabtree and Cramer demonstrated that oxygen was an essential element of the response of cells to irradiation in 1930. They have found that hypoxic cancer cells were 3 times resistant to irradiation when compared to the aerobic cells (19).

Although hypoxia has been extensively discovered in the context of cancer, vast majority of discoveries neglected the importance of the measurement of partial oxygen pressure within the tumor tissue. Physiologically, tissue oxygenation is dependent on metabolic demands and requirements of organs and can fluctuate accordingly. Growing body of literature have suggested that physiologic normoxia and atmospheric oxygen level are distinct notions and cannot be used interchangeably. Even though brain is one of well-perfused organs throughout the body, partial oxygen pressure of brain parenchyma was measured around 35 mmHg (4.6%) under normal circumstances (20). This value is nowhere near to atmospheric oxygen level, which is named normoxia (ie, 20% of oxygen). Not surprisingly, **in vitro** cell culture systems are performed in approximately 20% of oxygen. Whereas corresponding pO_2 values in human organs range between 1% to 11%. It is critical to recognize that misinterpretation complicated by the differences between physiological and atmospheric normoxia may result in misleading.

In the presence of oxygen, prolyl hydroxylase enzymes (PHD) hydroxylate the master transcriptional regulator of hypoxia (HIF1α), thereby rendering HIF1α susceptible for ubiquitination by VHL. Subsequently, ubiquitinated HIF1α is degraded by proteasomes. In contrast, PHD enzymes are inhibited in the absence of oxygen. Consequently, HIF1α molecules are stabilized and translocate to the nucleus to promote metastasis, cell survival, glycolysis, angiogenesis, and immune responses as depicted in Figure 1 (21). The state of insufficient oxygen availability is defined as hypoxia. In the presence of oxygen shortage, the cellular oxygen sensor proteins, prolyl hydroxylases (PHD), are inhibited, in turn, hypoxia-inducible factors translocate to the nucleus. Similar to the PHD proteins, under inadequate oxygen supply, FIH1

(factor inhibiting HIF1) function is inhibited, resulting in disruption of hydroxylation of asparagine residues and allowing for increased HIF transcriptional activity (21-25). On the other hand, T cells stimulated with cognate antigens and costimulatory molecules upregulate their HIF-1α expression via oxygen-independent mechanisms (26). Subsequently, hypoxia activates the NF-κB pathway. Surprisingly, in T cells, stimuli that activate NF-κB such as cognate antigen also induce the expression of HIF-1a protein. Upon TCR stimulation, HIF-1α protein stabilization occurs which can be reinforced by concurrent hypoxic exposure. In addition, IL-6 can induce HIF-1α stabilization in T cells. It is unclear whether it is related with coupling of TCR stimulation or increased oxygen consumption of activated T cells. Tumor hypoxia induces the chemokine CCL28 expression, which preferentially induces the recruitment of Treg cells. In addition, HIF-1α can induce the transcriptional activation of FoxP3, to promote the differentiation of Treg cells. VHL-deficient thymocytes constitutively express HIF-1α, resulting in detrimental effect on normal thymocyte development and differentiation. Moreover, removal of Ca from the cytoplasm via HIF1a-induced increase in SERCA2 Ca pumps following TCR cross-linking. HIF-1α defective T cells had increased cytokine production including IFNγ and IL-2. Besides its role in hypoxia, HIF-1α may have a crucial role in T cell activation and differentiation.

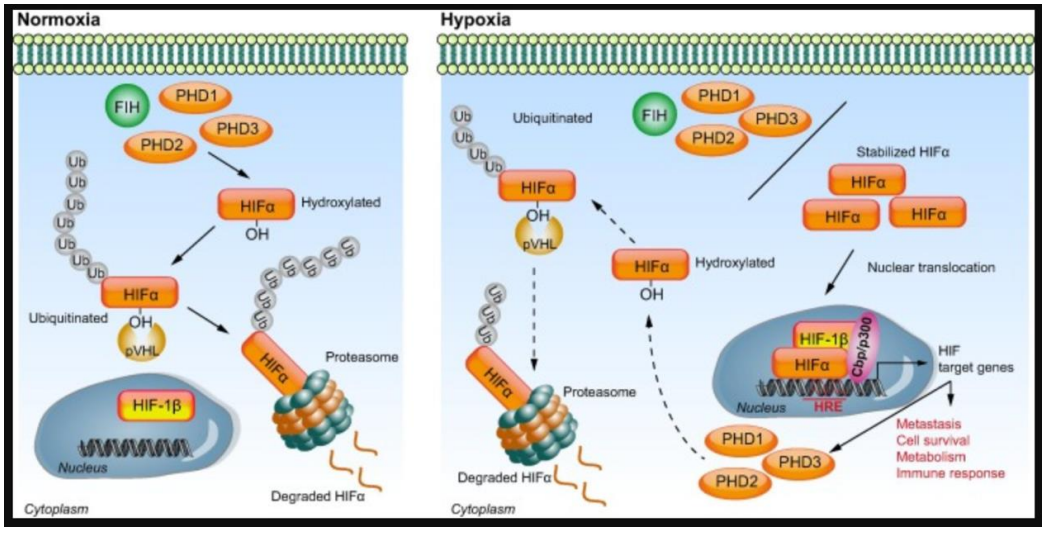

Figure 2.1. Oxygen dependent HIF signalling (Adapted from Wilson 2014 (21))

Hypoxic signal plays a fundamental role in vascular endothelial growth factor (VEGF)-induced angiogenesis. As the tumor growth outpaces the vasculature's capability to perfuse tumor microenvironment, master transcriptional regulator of hypoxic response (ie, HIF1α) increases glucose utilization of cancer cells through anaerobic glycolysis. On the other hand, greater glucose utilization by cancer cells results in glucose-depleted microenvironment for neighboring cells (eg, immune cells, fibroblasts, and endothelial cells).

Within 70 to 150 micron of tumor vasculature, rapidly dividing cancer cells consume vast majority of oxygen, thereby resulting in oxygen shortage for the tissue compartments further away from the vasculature. Thus, spatial and temporal heterogeneity in terms of oxygenation is inevitable within the tumor tissue.

Oxygen availability within tumors has a broad range of implications in cancer treatment including chemotherapy, radiation therapy, and recently immunotherapy.

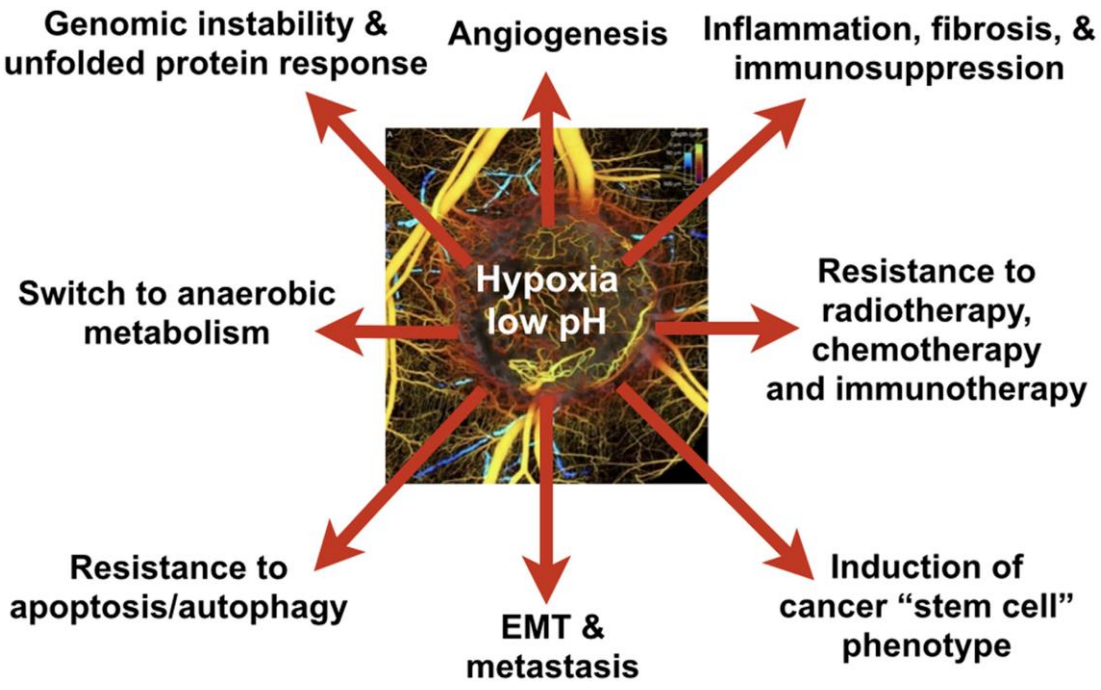

Figure 2.2. Hypoxia and Acidosis as a result of Impaired Perfusion Promote Tumor Development and Therapy Resistance (Adapted from Jain 2014 (27))

3. MATERIALS AND METHODS

3.1. Materials

3.1.1. Mouse breeding and tumor induction

Phd2$^{+/-}$ mice have been bred as previously described (5). Phd2$^{+/-}$ mice were provided by the laboratory of Massimiliano Mazzone. Tumor induction was performed subcutaneously (28). Mice matched for age and sex were used for the experiments. Phd2$^{+/-}$ mice were co-housed with controls whenever possible. Tumor volumes were calculated by the caliper. All mice were housed in Salk Institute Animal Resources Center in pathogen-free conditions. Each animal experiments were performed according to the approved protocols of the Salk Institute Animal Care and Use Committee. For tumor induction, YUMMER1.7 and MC38 cells were harvested at 60%–85% confluence. Cells were trypsinized with 0.25% trypsin for 1 min before deactivation with media containing 10% serum. They were then washed twice with sterile 1× PBS. Cancer cells were counted with an Invitrogen Countess or a hemocytometer. Cells resuspended in 100 µl of sterile PBS were inoculated subcutaneously into a shaved rear flank by using an insulin syringe.

3.1.2. Cell lines

YUMMER 1.7 murine melanoma cells were derived from YUMM cell lines which were obtained from *Braf*^{V600E}*Cdkn2a*$^{-/-}$ Pten$^{-/-}$ mice and subsequently irradiated three times (**Figure 2.1**). YUMMER 1.7 murine melanoma cells were gift from Marcus Bosenberg Lab at Yale University. YUMMER 1.7 murine melanoma cells were passaged in 1:1 DMEM F-12 supplemented with 1% L-glutamine, 1% non-essential amino acids, 10% FBS, and 1% penicillin-streptomycin (28). MC38 and murine melanoma cells were passaged in DMEM F-12 supplemented with 10% FBS. 2.1.7. In 500 mL DMEM F-12 media; 5 mL L-glutamine, 5 mL non-essential amino acids solution, 50 mL FBS (heat-inactivated), and 5 mL Pen/Strep added for the preparation of 10% cell culture media.

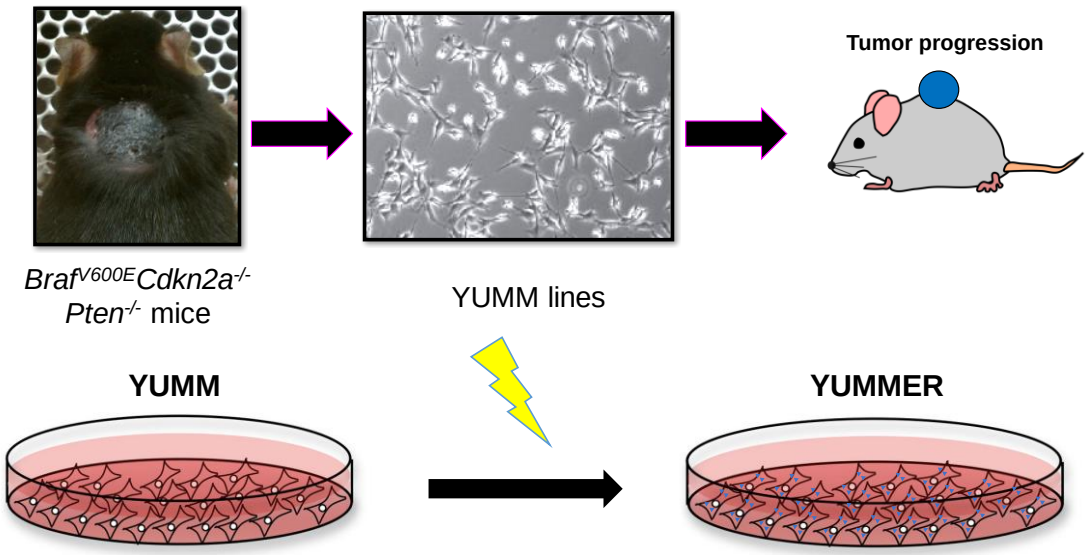

Figure 3.1. YUMMER 1.7 cell line

3.1.3. Cell Culture and RPMI Medium

DMEM F-12 supplemented with L-glutamine, high glucose, sodium pyruvate, and HEPES (Catalog # 11330057) and RPMI-1640 with HEPES buffer, L-glutamine, and high glucose (Catalog # A1049101) were purchased from ThermoFisher Scientific, USA. Non-essential amino acids solution (Catalog # 11140050), L-glutamine (Catalog # 25030-081) and Pen/Strep (5,000 units/mL Penicillin and 5,000 μg/mL Streptomycin; Catalog # 25070-063) were purchased from ThermoFisher Scientific, USA. Heat inactivated FBS (56° for 30-min; Catalog # 10082147) and 1X PBS (Catalog # 10010023) were also supplied from ThermoFisher Scientific, USA.

3.1.4. Flow cytometry reagents

Single-cell suspensions from harvested tissues (eg, tumors and spleens) were pre-incubated with anti-Fc receptor antibody (2.4G2) on ice for 15 min in complete RPMI with 10% serum. The cells were then stained with the desired antibodies on ice for 30 min. For the cytokine analysis, cells were fixed and permeabilized in buffer. They were then stained with antibodies to detect intracellular cytokines. For gating, compensation was performed with splenocytes before being manually confirmed and compared with previous experiments. Samples were acquired on LSRII flow

cytometers. Data were analyzed with Flowjo (Flowjo, LLC., Ashland, OR). Antibodies against CD45 (A20), CD8 (53-6.7), CD4 (GK1.5), CD11b (M1/70), Ly6C (HK1.4), Ly6G (1A8-Ly6G), PD-1 (29F.1812), and Foxp3 (FJK- 16s) were purchased from eBioscience. Antibodies against CD4 (RM4-5), F4/80 (BM8), PD-L1 (10F.9G2), TNF-α (MP6-XT22), and IFN-γ (XMG1.2) were supplied from Biolegend. LIVE/DEAD red was purchased from Invitrogen. Hypoxia staining was detected by intracellular staining of pimonidazole adduct (Hypoxyprobe).

3.1.5. Histology reagents

In some experiments, after pimonidazole pulsing, tumor tissues were dissected and fixed in 2% paraformaldehyde (PFA) at 4° C overnight and snap frozen in Optimal Cutting Temperature Compound (OCT) (Tissue-Tek). Tissue blocks were then sectioned (Cryostat microtome). Tissue was blocked in blocking buffer, stained with CD4 (RM4-5), CD8 (53-6.7), hypoxyprobe (Hypoxyprobe) and DAPI (Life Technologies). Inorder to avoid bleaching, sections were mounted with ProLong Diamond Antifade Mountant (Life Technologies). Sections were imaged with a Zeiss LSM 710 Laser Scanning Confocal Microscope and analyzed with ImageJ.

3.1.6. Tumor digestion and TIL analysis

21 days after tumor induction, when tumors reached the end point (1 or 2 cm^3 in each experiment), the mice were inoculated intraperitoneally with pimonidazole (80 mg/kg, Hypoxyprobe) in sterile PBS 1.5 hours prior to sacrifice (29). In some experiments, mice were also administered either control vehicle (isotype control), anti-CD4 (GK1.5 10 mg/kg every day), and anti-CD8 (TIB210 10 mg/kg every 3 days) for total of 10 treatments. Mice were sacrificed according to institutional guidelines. Tumor tissues and spleens were harvested and manually disrupted, and then digested in complete RPMI with 2% serum, 0.5 mg/ml collagenase IV, and 0.1 mg/mL DNase I in a 37°C incubator for 20 min. To remove debris, cell suspensions were filtered through a 70 μm cell strainer. To give the total number of the cells of interest, the percentage of the cells measured by flow cytometer is multiplied back against the

total cell count. This number is then divided by the tumor weight to calculate density (# cells per milligram of harvested tissue).

3.1.7. Immunofluorescence Staining

In some experiments, after pimonidazole pulsing, tumor tissues were harvested and fixed in 2% PFA at 4°C overnight and snap frozen at -80°C in OCT (Tissue-Tek). Tumors were sectioned 7 μm thickness in the Cryostat microtome at -°25C. Cut sections were blocked in blocking buffer at room temperature for 1 hour. All the reagents required to prepare blocking buffer were shown in Table 1. Fluorescence-labelled antibodies used for the immunofluorescence staining of tumor sections are listed in Table 2.

Table 3.1. Blocking buffer reagents

Name	Catalog #	Dilution
Bovine serum albumin	**PI37525**	**0.2%**
Sodium azide	**S2002**	**0.05%**
Triton	**X100**	**0.3%**
Rat serum	**31888**	**10%**
Purified mouse Fc block	**101302**	**1:100**

Table 3.2. Immunofluorescence Antibodies

Name	Clone	Dilution
Anti-mouse CD4	**RM 4-5**	**1:100**
Anti-mouse CD8	**53-6.7**	**1:100**
Pimonidazole	**Hypoxyprobe-1**	**1:200**

3.1.8. Flow Cytometry Instruments

Fluorescence-labeled antibodies used for the staining of the cells are listed in Table 3. Dilutions were done in FACS buffer (2% FBS in PBS). Cell activation cocktail (without Brefeldin A) was purchased from Biolegend (Catalog # 423302). Brefeldin A was purchased from Biolegend to stop cytokine release form Golgi organelle (Catalog # 420601). LSR II and FACSDiva v8.0.1 (BD Biosciences, USA) software were used for the data acquisition. Data were analyzed by using FlowJo v10 (BD Biosciences, USA).

Table 3.3. Flow Cytometry Antibodies

Name	Clone	Company	Dilution
Anti-mouse CD45	**A20**	**eBioscience**	**1:500**
Anti-mouse CD8	**53-6.7**	**eBioscience**	**1:400**
Anti-mouse CD4	**GK1.5**	**eBioscience**	**1:400**
Anti-mouse CD11b	**M1/70**	**eBioscience**	**1:200**
Anti-mouse Ly6C	**HK1.4**	**eBioscience**	**1:200**
Anti-mouse CD16/32	**93**	**Biolegend**	**1:1000**
Name	Clone	Company	Dilution
Anti-mouse Ly6G	**1A8-Ly6G**	**eBioscience**	**1:200**
Anti-mouse PD-1	**29F.1812**	**eBioscience**	**1:200**
Anti-mouse FoxP3	**FJK-16s**	**eBioscience**	**1:100**
Anti-mouse CD4	**RM4-5**	**Biolegend**	**1:400**
Anti-mouse F4/80	**BM8**	**Biolegend**	**1:200**
Anti-mouse PD-L1	**10F.9G2**	**Biolegend**	**1:200**
Anti-mouse TNF-α	**MP6-XT22**	**Biolegend**	**1:100**
Anti-mouse IFN-γ	**XMG1.2**	**Biolegend**	**1:100**
Anti-mouse LAG3	**125221**	**Biolegend**	**1:200**
Anti-mouse CD38	**102728**	**Biolegend**	**1:200**
Anti-mouse CD39	**143806**	**Biolegend**	**1:200**
Pimonidazole	HP2-200	**Hypoxyprobe**	**1:500**

3.2. Methods

3.2.1. Animals

4 to 8 weeks old wild type or *PHD2*$^{+/-}$ adult male C57BL/6 littermate mice were housed in the Salk Institute Animal Facility under the controlled ambient conditions (22$\pm$2°C) regulated with 12-hour light/dark cycles. Mice were provided with sufficient food and water. All procedures were conducted in accordance with the ethical guidelines for the care and use of laboratory animals and approved by Animal Care and Use Committee (ACUC) of the Salk Institute.

3.2.2. Tumor induction

4 to 8 weeks old wild type or *PHD2*$^{+/-}$ adult male C57BL/6 littermates were subcutaneously injected with 0.5 x 10^6 YUMMER 1.7 murine melanoma cells in 100 μL sterile PBS by using insulin syringe. For the consistent and ideal tumor growth, the cells that injected should be at 70-80% confluence at the day of tumor induction.

3.2.3. Pimonidazole pulsing

To image tumor hypoxia, pimonidazole in PBS was administered intraperitoneally (80 mg/kg) to the mice 90-min prior to euthanasia. Subsequently, tumor hypoxia was imaged by staining with FITC-labelled anti-pimonidazole antibody (Hypoxyprobe). Pimonidazole is reductively activated in live hypoxic cells and forms stable adducts. Monoclonal antibody against Pimonidazole binds to these adducts enabling hypoxia detection by immunofluorescence staining.

3.2.4. Staining for surface and intracellular proteins for flow cytometry analysis

Staining of the mouse samples were performed on the 96-well plates. Cells were resuspended at 1x 10^6/mL in the 10% RPMI media. Samples were centrifuged at 1500 rpm for 5 minutes. Cells were then resuspended in 100 μL staining buffer containing the fluorescent-labeled antibodies and anti-mouse CD16/32 as listed in Table 2 and incubated at 4°C for 30 minutes. Samples were washed with 100 μL of FACS buffer and centrifuged at 1500 rpm for 2 minutes. Flow cytometry staining was performed under dark condition to prevent quenching.

For intracellular cytokine staining, cells were pre-incubated with cell stimulation cocktail without Brefeldin A at 37°C for 30 minutes. Cell activation cocktail without Brefeldin A was diluted 1:500 in 10% RPMI media. After stimulation, cells were incubated with an additional 100 μL of Brefeldin A and cell activation cocktail mixture for $4^{1/2}$ hours. Brefeldin A and cell activation cocktail were diluted 1:500 in 10% RPMI media. Cells were centrifuged at 1500 rpm for 2 minutes and washed with 1X PBS to remove Brefeldin A and cell activation cocktail. This step was followed by surface staining as described above. Following to surface staining, cells were incubated with 1:3 dilutions of the Fix/Perm concentrate (Catalog # 00-5123-43 eBioscience, USA) and Fix/Perm diluent (Catalog # 00-5223-56 eBioscience, USA) at 4°C for 30 minutes. Cells were then washed with 1X Permeabilization buffer (Catalog # 00-8333-56 eBioscience, USA). Following permeabilization, cells were centrifuged at 1500 rpm for 5 minutes. 10X Permeabilization buffer was diluted in distilled water.

Subsequently, cells were resuspended in 100 μL permeabilization buffer containing the fluorescence-labeled or appropriate isotype control antibodies as listed in Table 2 and incubated at 4°C for 30 minutes. To remove unbound antibodies, cells were washed with 1X Permeabilization buffer. Consequently, cells were resuspended with 200 μL FACS buffer. As a negative control, unstimulated cells were incubated with Brefeldin A in 1:1000 dilution without prior cell activation step.

Single stained samples were prepared with Compensation Beads (Catalog # 01-2222-42 eBioscience, USA) for each fluorochrome used in the staining of the samples. Unstained controls were prepared from fixed mouse splenocytes. These controls were used to set Voltages and compensations adjusted by using these single stained beads and unstained splenocytes. Acquired event number was between 100,000-1,000,000 for mouse samples.

3.2.5. Statistics

Statistical analyses of the data were performed by using GraphPad Prism 6.0c. Student's two-tailed t-tests was used to compare two different groups. Differences between more than 2 groups were assessed by One-Way ANOVA test.

For vessel elongation studies, statistical analyses were done on log-transformed data of length of single blood vessels. Tumor sizes were measured by caliper. Three dimensions were taken for the calculation of tumor volume. Equation used in the calculation of tumor volume: 0.5 * L*W*H.

4. RESULTS

4.1. Immunofluorescence staining of CD31 in *PHD2* haplodeficient mice with YUMMER 1.7 tumors.

Immunofluorescence staining of the sections for CD31, which is an endothelial cell marker, revealed that WT tumors induce punctuated, disorganized, and discontinuous blood vessel formation. Whereas, in *PHD2*$^{+/-}$ mice, the wall of blood vessels was demarcated with clearly defined boundaries and continuous alignment. In turn, these changes resulted in a more regular vessel structure (**Figure 4.1 A and B**). Quantification of maximum elongation demonstrated that blood vessels in *PHD2*$^{+/-}$ mice were significantly more elongated than the blood vessels in WT mice (**Figure 4.1 C**).

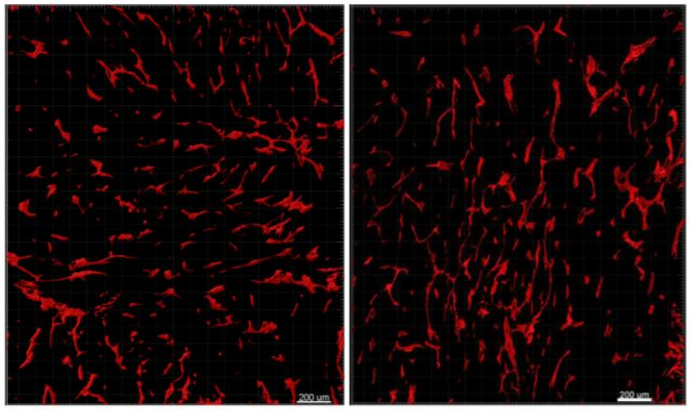

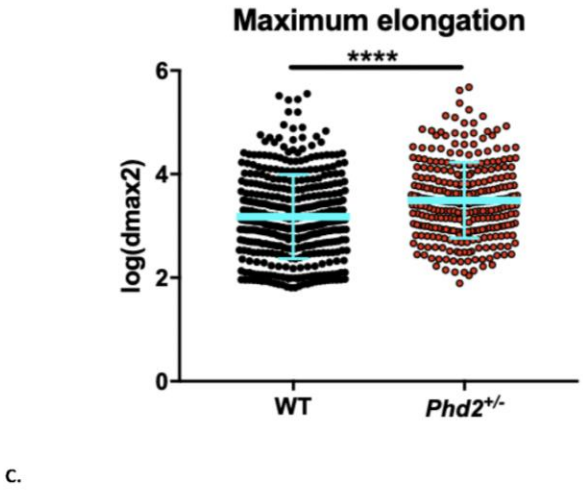

Figure 4.1. Effect of *PHD2* haplodeficiency on vessel elongation in mice with YUMMER 1.7 melanoma tumors. WT and *PHD2*$^{+/-}$ littermates were induced with 0.5 x 10^6 YUMMER 1.7 murine melanoma cells. At day 21 after tumor induction, tumor tissues were harvested and fixed in 2% PFA at 4°C overnight and snap frozen at -80°C in OCT (Tissue-Tek). Tumors were sectioned 7 μm thickness in the Cryostat microtome at -°25C. Cut sections were stained for CD31 (red). *; p<0.05, **; p<0.01; ***; p<0.001, ****; p<0.0001

4.2. Assessment of vessel maturation in PhD2 haplodeficient mice via immunofluorescence staining of VE-Cadherin

To investigate whether tumor vessels are more mature and tighter in *PHD2*$^{+/-}$ mice, VE-Cadherin staining was performed. Cut tumor sections were stained for VE-Cadherin, which is a maturation marker for endothelial cells. The tumor vessels covered by VE-Cadherin^{+} cells were more prevalent in *PHD2*$^{+/-}$ mice (Figure 4.2 A and B). These findings demonstrated that PhD2 haplodeficiency promotes blood vessel maturation and elongation.

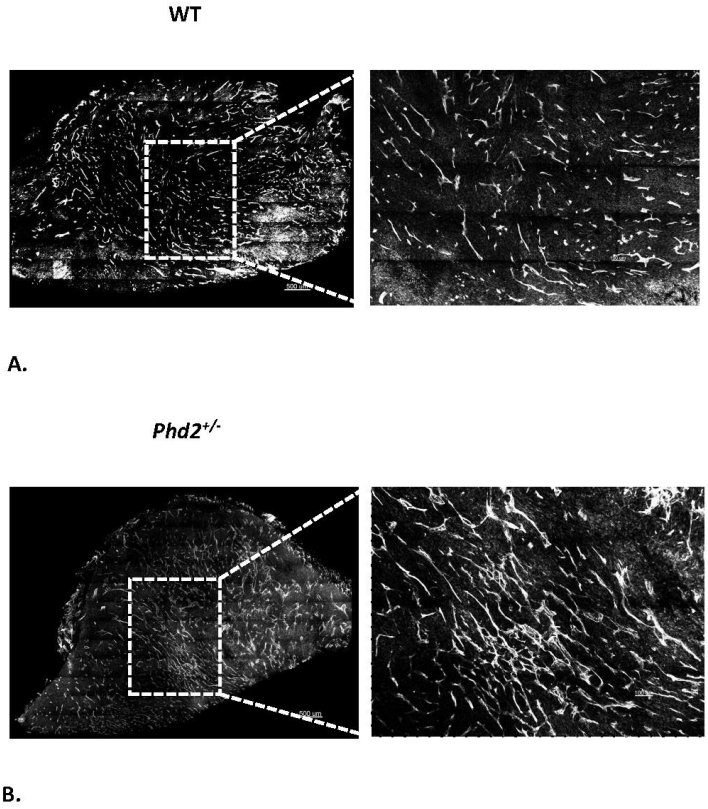

Figure 4.2. Impact of Phd2 haplodeficiency on vessel maturation in mice with YUMMER 1.7 melanoma tumors. WT and *PHD2*$^{+/-}$ littermates were induced with 0.5 x 10^6 YUMMER 1.7 murine melanoma cells. At day 21 after tumor induction, tumor tissues were harvested and fixed in 2% PFA at 4°C overnight and snap frozen at -80°C in OCT (Tissue-Tek). Tumors were sectioned 7 μm thickness in the Cryostat microtome at -°25C. Cut sections were stained for VE-Cadherin (white).

4.3. Investigation of pericyte-coverage and tight junction in *PHD2*$^{+/-}$ mice

The above findings suggest that phenotypic features of tumor vessels of WT and *PHD2*$^{+/-}$ mice are distinct. To further confirm this finding, cut tumor sections were stained with CD146, CD31, and α-smooth muscle actin (α-SMA) antibodies. As shown in Figure 4.3 A and B, co-staining of CD146, CD31, and α-SMA was observed in *PHD2*$^{+/-}$ mice. Whereas, in WT mice, tumor vessel was not stained for CD146, which is an indicator of cell-cell interaction between endothelial cells (30).

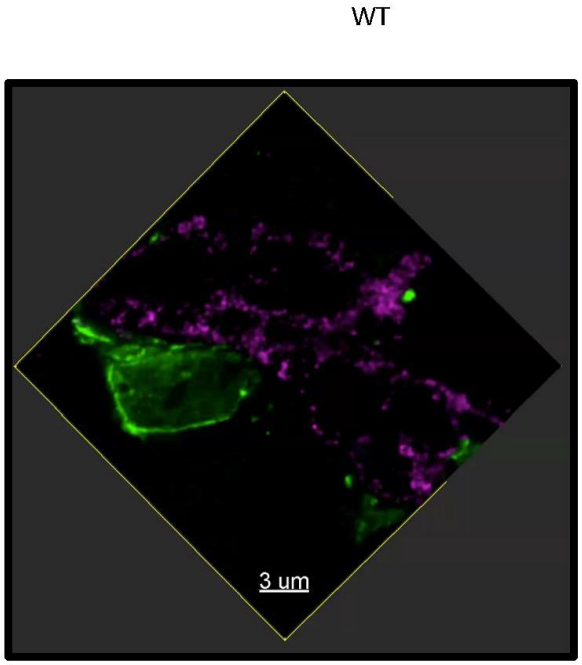

A.

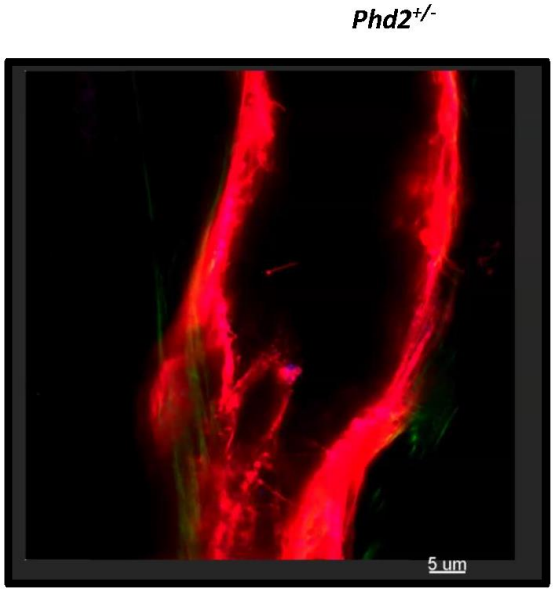

B.

Figure 4.3. Effect of *PHD2* haplodeficiency on vessel normalization in mice with YUMMER 1.7 melanoma tumors. WT and *PHD2*$^{+/-}$ littermates were induced with 0.5 x 10^6 YUMMER 1.7 murine melanoma cells. At day 21 after tumor induction, tumor tissues were harvested and fixed in 2% PFA at 4°C overnight and snap frozen at -80°C in OCT (Tissue-Tek). Tumors were sectioned 7 μm thickness in the Cryostat microtome at -°25C. Cut sections were stained for CD146 (red), CD31 (purple), and α-SMA (green).

4.4. Analysis of immune infiltration within hypoxic and normoxic tumor regions

To analyse hypoxic localization of $CD4^+$ and $CD8^+$ T cells, mice with established subcutaneously grown YUMMER 1.7 tumors were pulsed with Hypoxyprobe-1 (80 mg/kg). After 90 minutes of labeling, tumors were fixated in 2% PFA and snap-frozen. Subsequently, 7 μm cryosections were prepared and immunofluorescence staining was performed. For tumor infiltrating lymphocyte analysis, cut tumor sections were stained with pimonidazole, CD4+, and CD8+ antibodies. Using a molecular in vivo hypoxia marker (i.e hypoxyprobe), Figure 4.4 A and B demonstrate that $CD4^+$ T cells were excluded from hypoxic tumor regions. Tumor infiltrating $CD4^+$ T cells preferentially localized within non-hypoxic tumor regions. Statistical comparison between hypoxic and non-hypoxic locations of CD4+ T cells seen in the representative images in Figure 4.4 A and B (scale bar, 150 μm) is shown in the histogram in Figure 4.4 C. As shown in Figure 4.4 D and E, similar to CD4+ T cell localization, CD8+ T cells were excluded from hypoxic tumor regions. Statistical comparison between hypoxic and non-hypoxic locations of CD8+ T cells seen in the representative images in Figure 4.4 D and E (scale bar, 150 μm) is shown in the histogram in Figure 4.4 F.

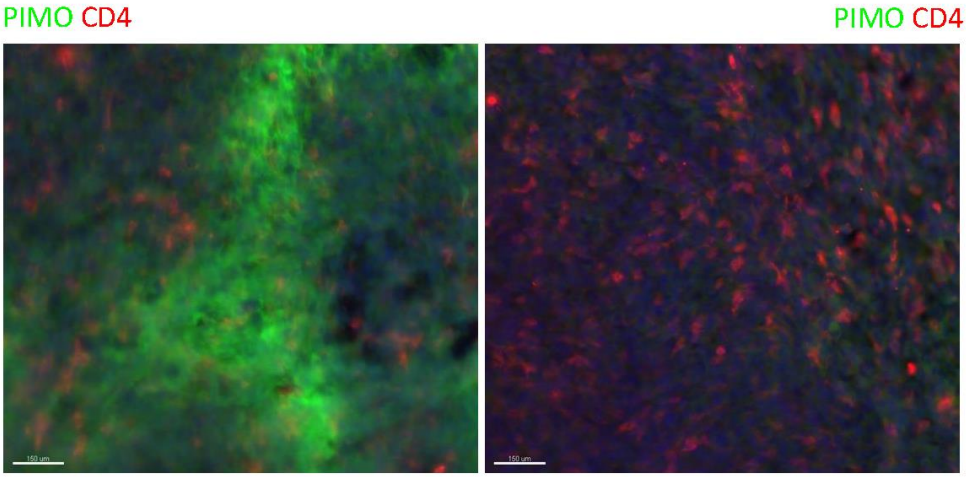

Hypoxic tumor region

Non-hypoxic tumor region

A.

B.

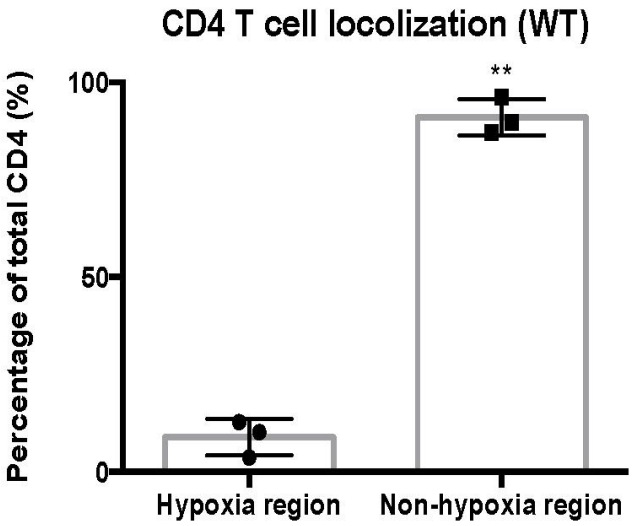

C.

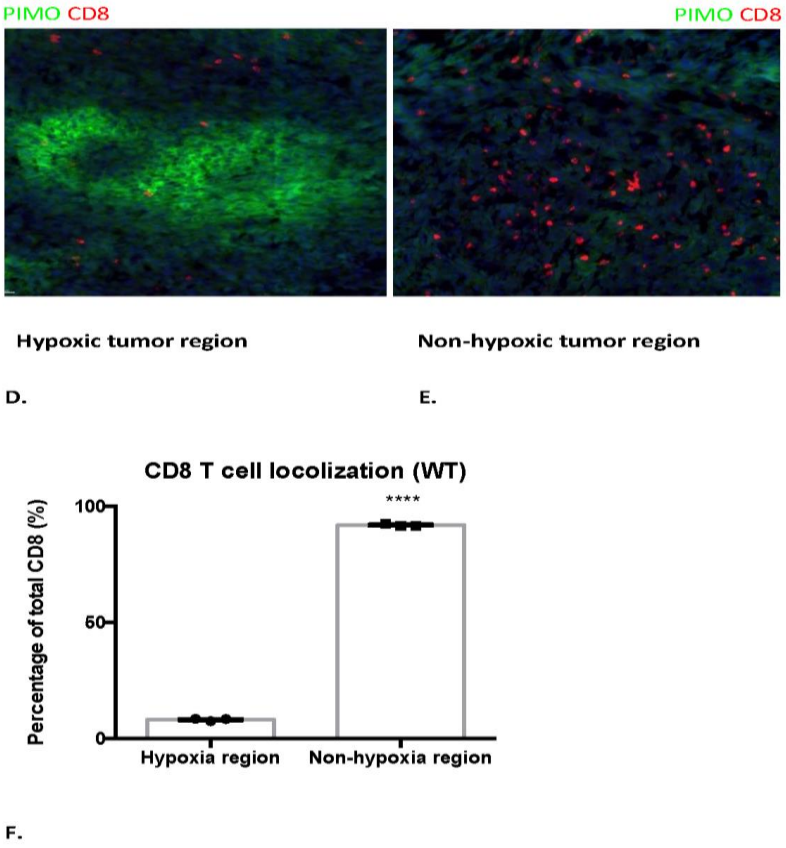

Figure 4.4. Immunofluorescence staining of tumor infiltrating lymphocytes within hypoxic and normoxic tumor locations. Representative images show exclusion of anti-tumor T cells from hypoxic tumor regions. After in vivo labeling of hypoxic tissue regions by 80 mg/kg of Pimonidazole, cut tumor sections were stained with 1:200 dilution of FITC-conjugated pimonidazole antibody (green). Anti-tumor T cell infiltration was examined by staining with 1:100 dilution of fluorescence conjugated anti-mouse CD4+ and CD8+ antibodies (red). n=3 mice. *; $p<0.05$, **; $p<0.01$; ***; $p<0.001$, ****; $p<0.0001$

4.5. Analysis of anti-tumor T cell infiltration in PHD2$^{+/-}$ and WT mice.

Having observed that *PHD2* haplodeficiency improved vessel structure and diminished hypoxia within tumors, comparison of T cell infiltration was performed by immunofluorescence staining. Above findings confirmed that CD4+ and CD8+ T cells were excluded from poorly oxygenated tumor regions. In parallel to these findings, improved CD8+ T cell infiltration was observed in *PHD2*$^{+/-}$ mice (Figure 4.5 A and B). Background staining was assessed by appropriate isotype control staining (Figure 4.5 C). Quantification of CD8^{+} T cells in WT and *PHD2*$^{+/-}$ mice indicated that vessel

normalization facilitated CD8+ T cell infiltration in *PHD2*$^{+/-}$ mice (Figure 4.5 D). Similarly, CD4+ T cell staining was performed (Figure 4.5 E and F) along with appropriate isotype control staining (Figure 4.5 G). Although there was a slight increase in CD4+ T cell infiltration in *PHD2*$^{+/-}$ mice compared to WT mice, the difference was not significant (Figure 4.5 H).

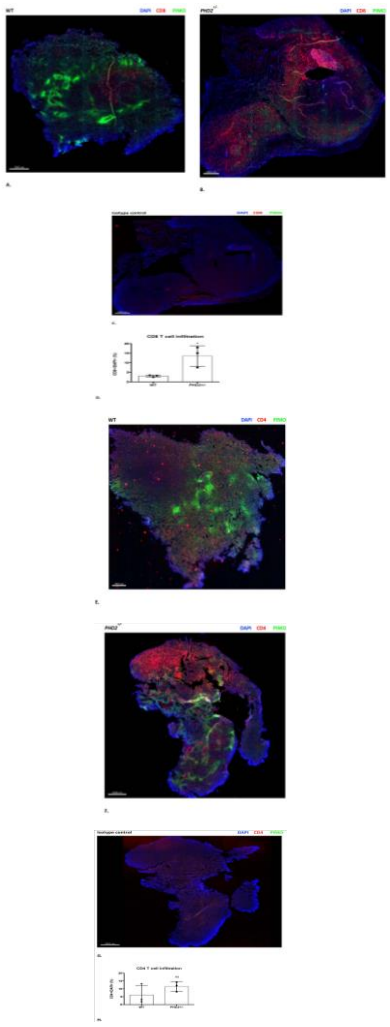

Figure 4.5. Immunofluorescence staining of T cells in WT and *PHD2*$^{+/-}$ mice. Representative images show improved infiltration of CD4 and CD8 T cells. After in vivo labeling of hypoxic tissue regions by 80 mg/kg of Pimonidazole, cut tumor sections were stained with 1:200 dilution of FITC-conjugated pimonidazole antibody (green). Anti-tumor T cell infiltration was examined by staining with 1:100 dilution of fluorescence conjugated anti-mouse CD4+ and CD8+ antibodies (red). n=3 mice.

4.6. Assessment of T cell dependency of tumor growth in PHD2$^{+/-}$ mice.

YUMMER 1.7 murine melanoma tumors are responsive to immunotherapy due to their high immunogenicity (28). To determine whether or not haplodeficiency of PHD2 has an impact on tumor growth, we injected 0,5 x 10^6 YUMMER 1.7 cells into WT and PHD2+/- littermates subcutaneously and then monitored tumor growth by caliper every 3 days. We found that tumors injected into PHD2+/- mice are substantially smaller than WT (**Figure 4.6 A and C**). This data was supported by tumor

weight. Data pertaining to tumor weight was pooled from 5 independent experiments as shown in different color (**Figure 4.6 B**). To better understand the role of T cells in PHD2+/- mice, we depleted both CD4+ and CD8+ cells by in vivo blocking antibodies and demonstrated that delayed tumor growth depends on T cells (**Figure 4.6 D and E**).

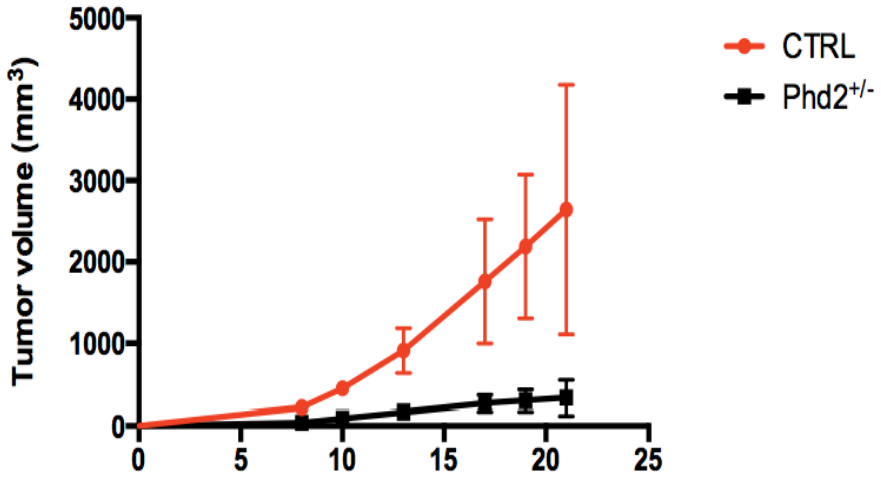

A.

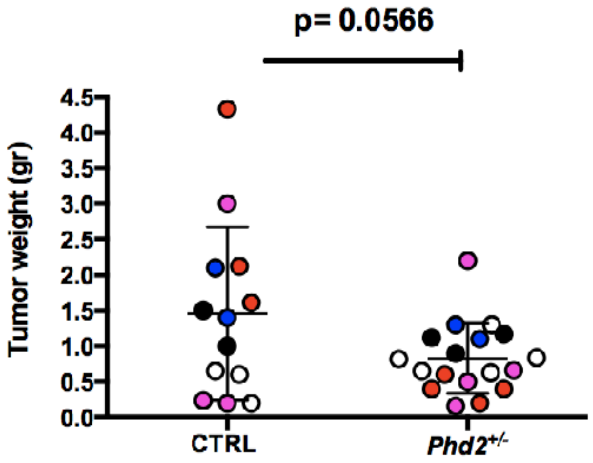

B.

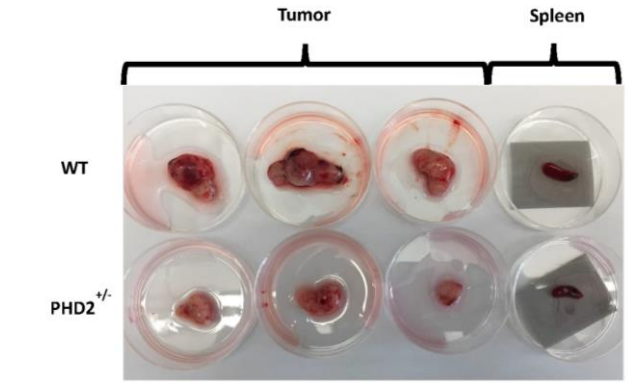

C.

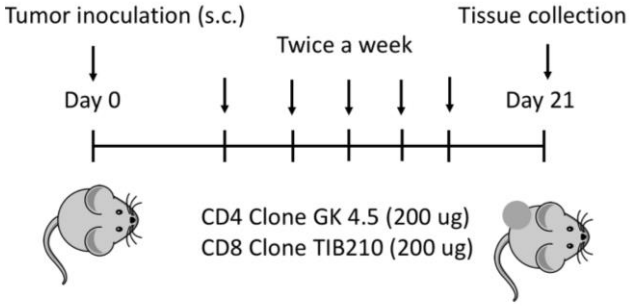

D.

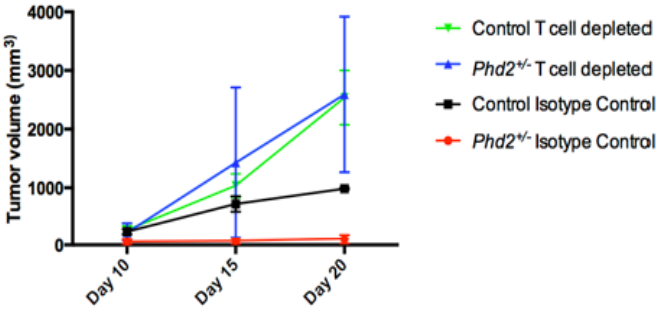

E.

Figure 4.6. Vessel normalization delays tumor growth in *PHD2*$^{+/-}$ mice in a T cell dependent manner. Tumor measurements of age-matched male PHD2+/- and WT littermates inoculated with 0,5 x 10^6 YUMMER 1.7 murine melanoma cells. The data is representative of five independent experiments. Mice inoculated with YUMMER 1.7 cells began receiving 200 ug CD4+ (GK 4.5) and CD8+ (TIB210) T cell depletion antibodies twice a week starting on day 7. The data represents one experiment (n=3). Each color represented independent experiments. Matched experiments are indicated by the same color.

4.7. Quantitative analysis of tumor infiltrating T cells in PHD2$^{+/-}$ and WT mice.

Mice bearing 21-day pre-implanted YUMMER 1.7 tumors are sacrificed and then tumor infiltrating immune cells are isolated. Total cell # is determined by Accuri cell counting and normalized to tumor weight. CD8+ T cell density is calculated by dividing total live cell # to tumor weight (**Figure 4.7 A**). CD4+ T cell density is measured by dividing total live cell # to tumor weight (**Figure 4.7 B**) Our data suggested that disruption of tumor hypoxia promotes CD4+ and CD8+ T cell infiltration within melanoma tumors in mice.

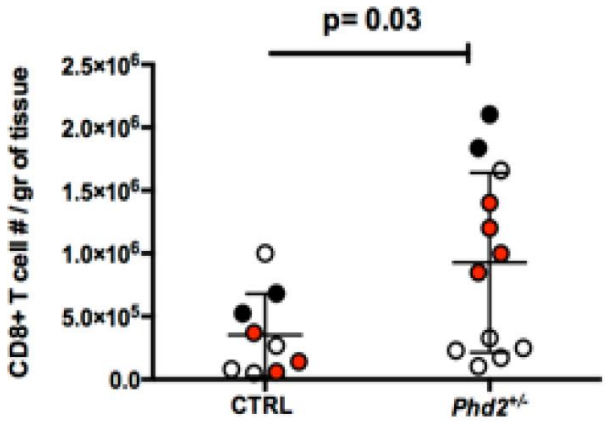

A.

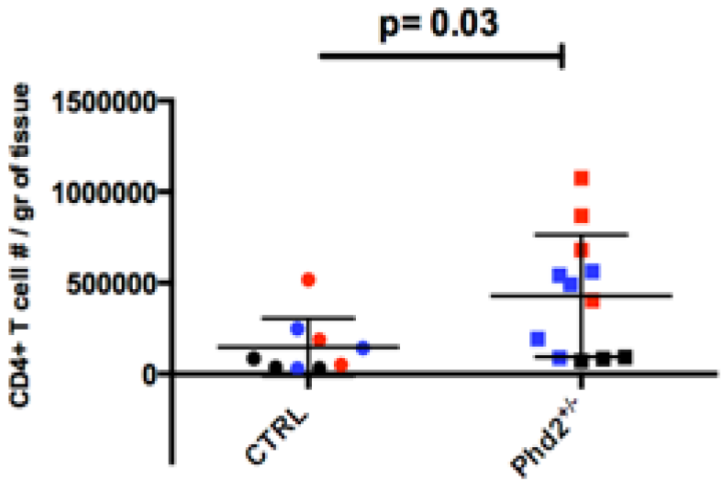

B.

Figure 4.7. Disruption of hypoxia promotes T cell infiltration within melanoma tumors. CD4+ and CD8+ T cell densities of PHD2+/- and WT littermates inoculated with 0,5 x 10^6 YUMMER 1.7 murine melanoma cells. Following to tumor isolation, tumors are weighed and total live cell # is counted by Accuri. Total CD4+ and CD8+ T cell numbers are calculated according to % of cells measured by flow cytometry and total live cells counted by Accuri. Density is calculated by dividing total CD4+ and CD8+ T cell # to tumor weight. Each color represented independent experiments. Matched experiments are indicated by the same color.

4.8. Characterization of T cell phenotype in PHD2$^{+/-}$ and WT mice

After demonstrating delayed tumor growth via reduced hypoxia, we sought to determine the impact of disruption of hypoxia on tumor infiltrating lymphocytes (TILs) in vivo. It has been previously uncovered by our lab and others that T cells in the TME are metabolically disadvantage and there has been a metabolic tug-of-war between cancer cells and immune cells (31, 32). Flow cytometry analysis of CD8+ T cells (CTLs) from PHD2+/- and CTRL mice bearing YUMMER 1.7 melanoma tumors revealed that exhaustion markers on CTLs such as PD-1, Lag-3, CD38, and CD39 were unaltered (**Figure 4.8 A and B**). These markers on TILs may indicate not only exhaustion state but also activation state of TILs, thereby we then asked whether cytokine production could be rescued by hypoxia reduction (33). Exhaustion is not a fixed term; however, it could be better examined by functional markers like proliferation and functionality (34).

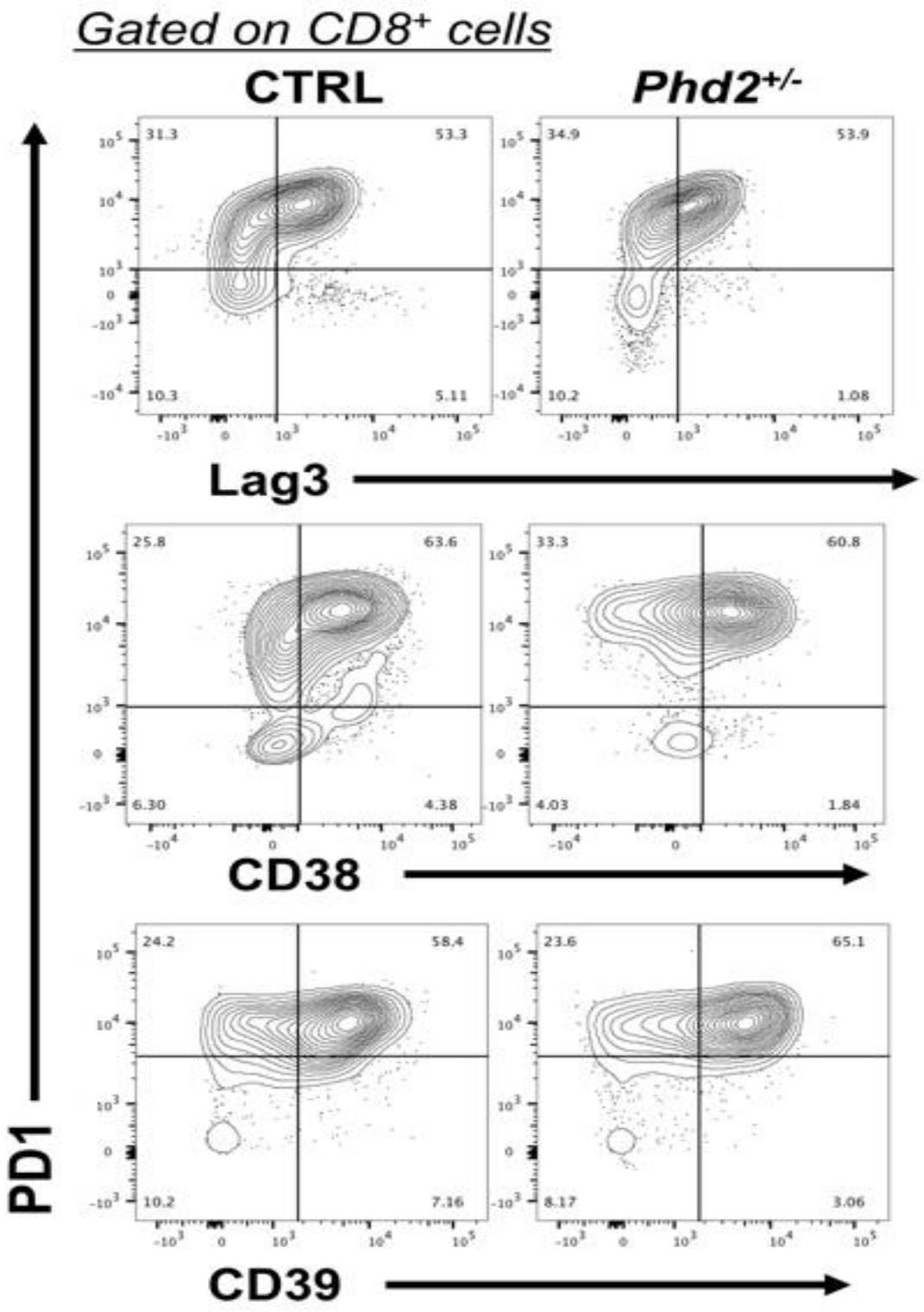
Gated on CD8+ cells
CTRL
Phd2+/-
31.3
53.3
10.3
5.11
34.9
53.9
10.2
1.08
Lag3
25.8
63.6
6.30
4.38
33.3
60.8
4.03
1.84
CD38
24.2
58.4
10.2
7.16
23.6
65.1
8.17
3.06
CD39
PD1

A.

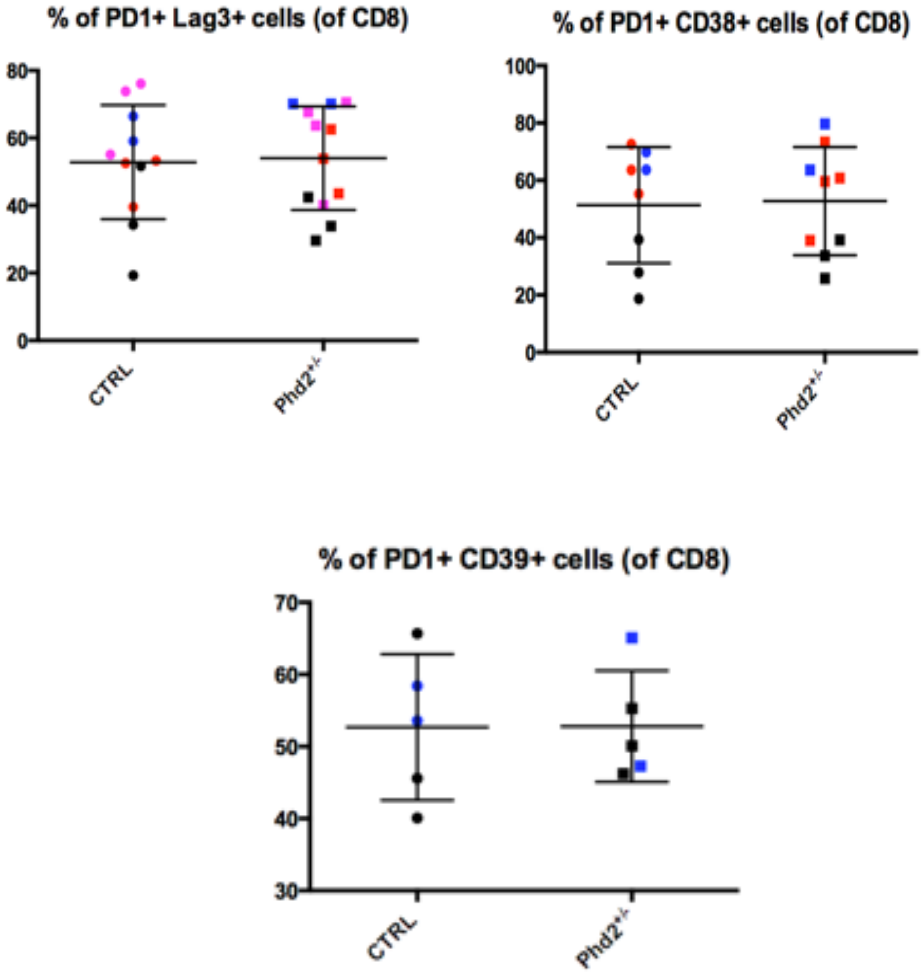

B.

Figure 4.8. Improving oxygenation through blood vessel normalization does not alter T cell phenotypes in melanoma tumors. Representative flow cytogram depicting PD-1, Lag-3, CD38, and CD39 expression on TILs from YUMMER 1.7 bearing mice. Quantification of PD-1, Lag-3, CD38, and CD39 expression on TILs. Data are pooled from at least six independent experiments. Each color represented independent experiments. Matched experiments are indicated by the same color.

4.9. Functional analysis of T cells in PHD2$^{+/-}$ and WT mice

Although tumor burden is significantly reduced due to improved oxygenation, we could not detect significant difference in terms of expression of exhaustion markers. Nonetheless, exhaustion is not only defined by surface markers instead, it is a reversible state of cells and should be determined along with functionality. In order to better understand whether infiltrated T cells are functional, we examined cytokine production of TILs. CD8+ T cells infiltrating PHD2+/- mice exhibit partially improved IFNγ production (**Figure 4.9 A and C**). However, the percentage of IFNγ+ TNFα+ CD8+ T cells was unaltered. (**Figure 4.9 B and C**). The data are pooled from three independent experiments.

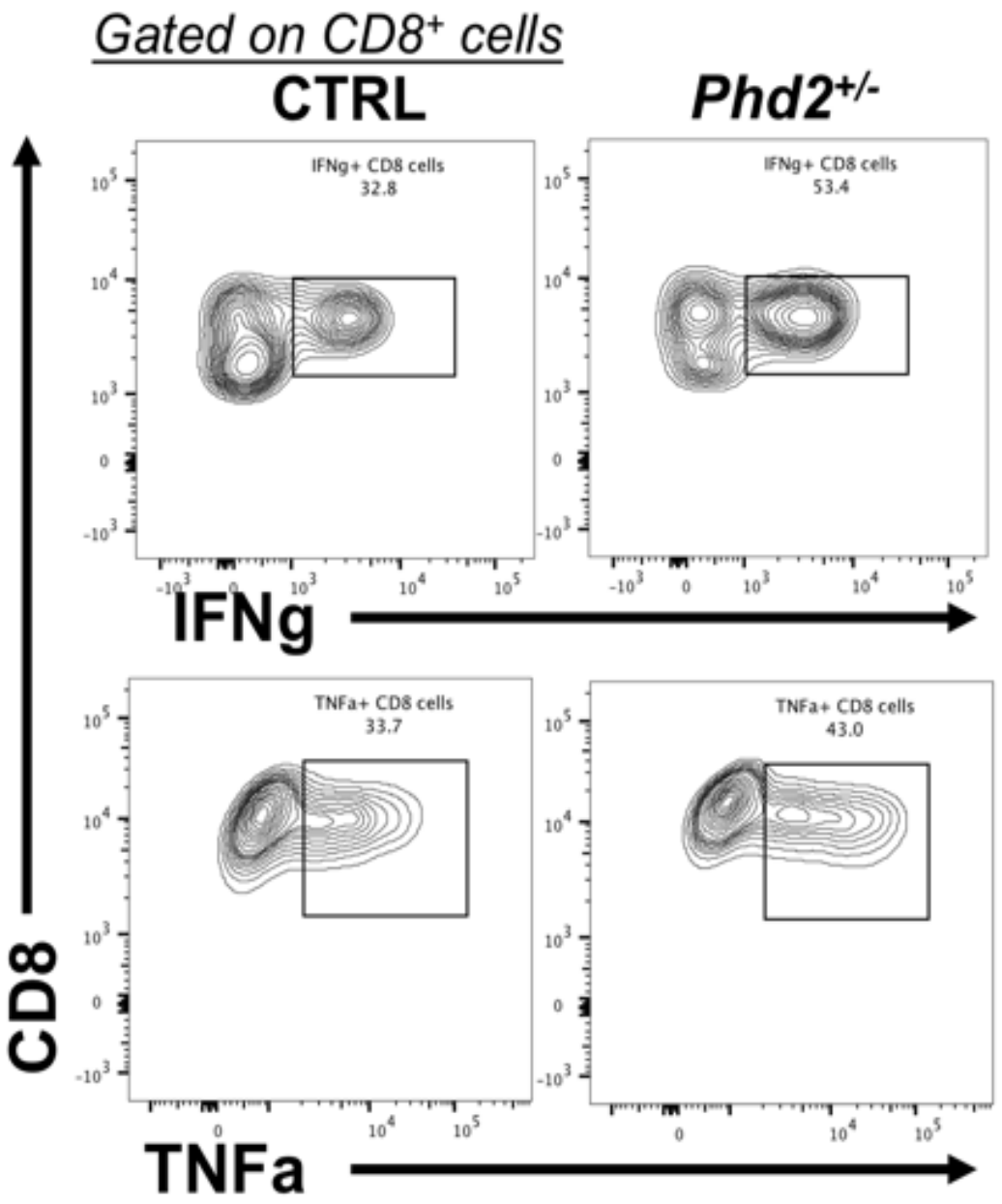
Gated on CD8+ cells
CTRL
Phd2+/-
IFNg+ CD8 cells
32.8
IFNg+ CD8 cells
53.4
IFNg
TNFa+ CD8 cells
33.7
TNFa+ CD8 cells
43.0
CD8
TNFa

A.

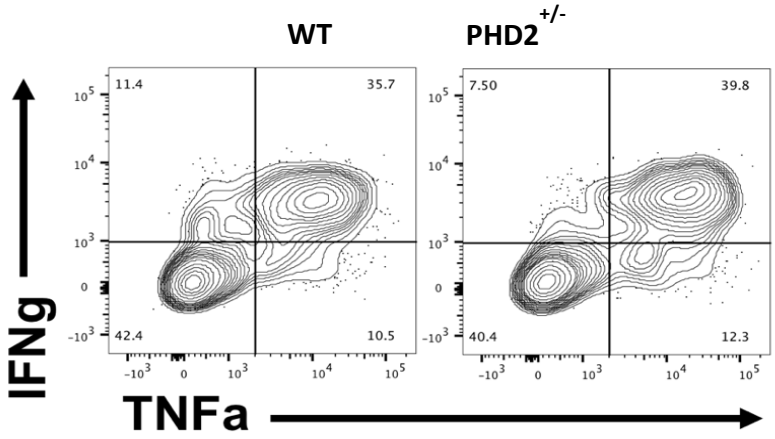

B.

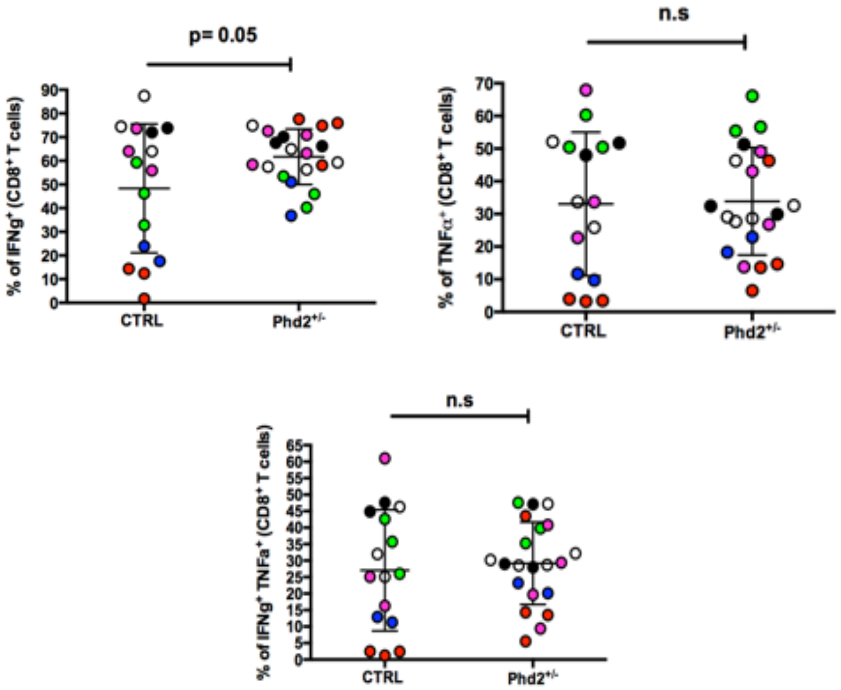

C.

Figure 4.9. Hypoxia reduction by haplodeficiency of PHD2 helps unleash IFNγ production of TILs. Representative flow cytogram depicting IFNγ and TNFα production of $CD8^+$ T cells. IFNγ production by CD8+ T cells is partially rescued by mitigation of hypoxia. Intriguingly, neither percentage of $TNF\alpha^+$ $CD8^+$ T cells nor $IFN\gamma^+$ $TNF\alpha^+$ double producers significantly altered. Each color represented independent experiments. Matched experiments are indicated by the same color.

4.10. Dissecting tumor associated macrophage infiltration by hypoxia ablation via PHD2 haplodeficiency.

We then sought to dissect the effect of diminished hypoxia on myeloid cell composition within melanoma tumors. As previously described, cancer cells recruit immature myeloid cells and force them differentiate into suppressive TAMs and MDSCs (35). This polarization is mediated by factors enriched within less oxygenated tumor regions. We hypothesized that disruption of hypoxia via blood vessel normalization might compromise the capacity of melanoma tumors to recruit anti-inflammatory macrophages. To test this hypothesis, we established 21-day YUMMER 1.7 melanoma tumors, and then examined the frequency of pro and anti-inflammatory macrophages. We demonstrated that CD11b+ Ly6G- F4/80+ myeloid cells are abundant in melanoma tumors obtained from CTRL mice (**Figure 4.10 A and B**). F4/80^{hi} myeloid cells within melanoma tumors show suppressive features and their abundance is associated with accelerated tumor growth (10). Nevertheless, improved oxygenation partially lowered F4/80^{hi} myeloid cell recruitment in melanoma tumors. On the other hand, M1-like proinflammatory macrophages are scarce in tumors. Even though their abundance is relatively smaller than TAMs, they may help recruit, differentiate, and activate CD4+ as well as CD8+ T cells through cytokines. We demonstrated herein profoundly increased infiltration of CD11b+ Ly6G- Ly6C+ pro-inflammatory macrophages in given tumor model (**Figure 4.10 A, B, and C**). This data may explain increased CD4+ and CD8+ T cell infiltration in tumors harvested from PHD2+/- mice.

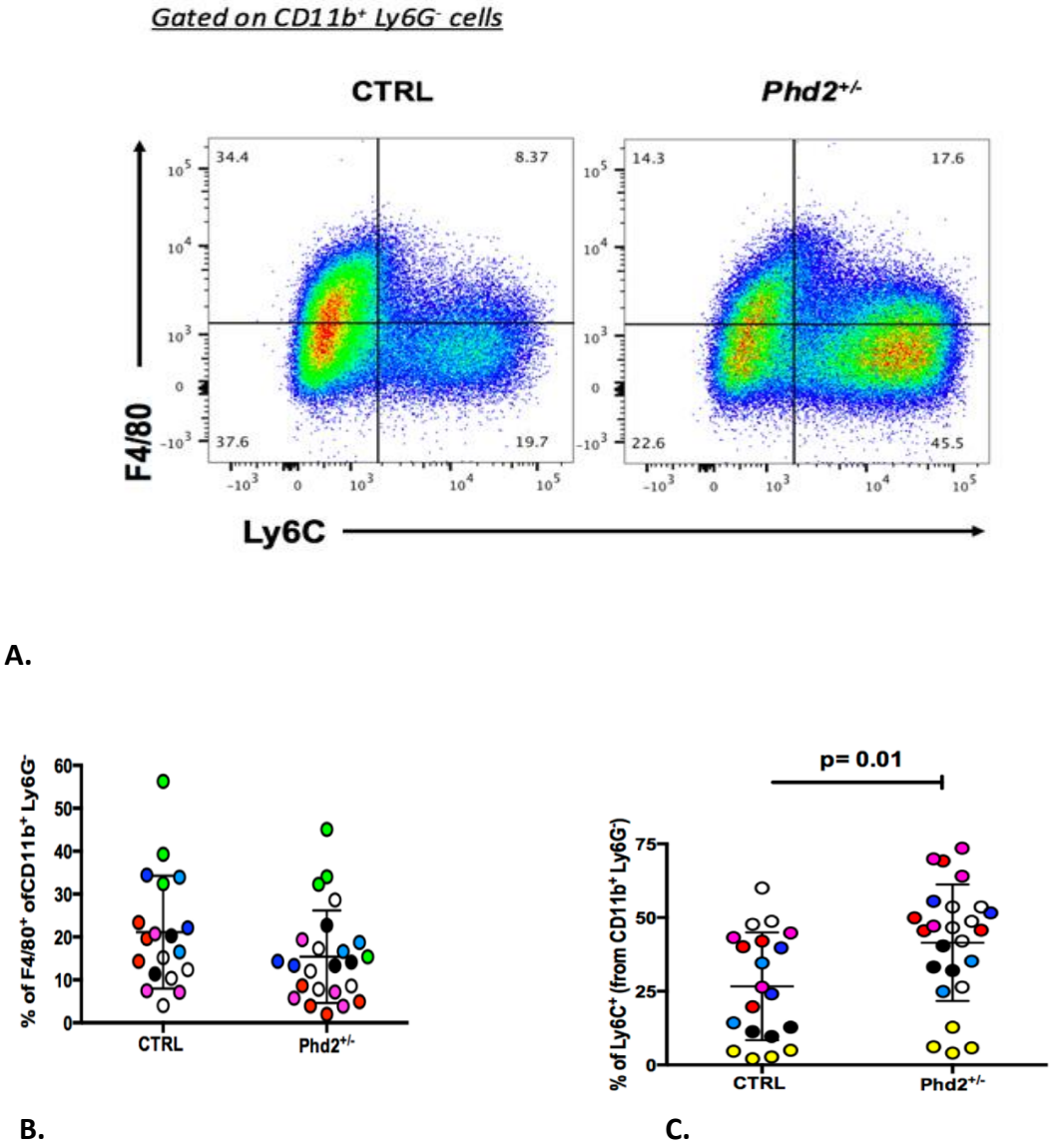

Figure 4.10. Hypoxia ablation impairs the infiltration of M2-like tumor promoting macrophages, however promotes inflammatory macrophage infiltration into melanoma tumors. Representative flow cytogram depicting the expression of F4/80 and Ly6C on $CD11b^+$ $Ly6G^-$ $CD45^+$ cells. Quantification of F4/80+ and Ly6C+ myeloid cells. Each color represented independent experiments. Matched experiments are indicated by the same color.

4.11. Analysis of PD-L1 expression on myeloid cells in PHD2$^{+/-}$ and WT mice.

PD-1 expressing CD8+ T cells engage with PD-L1+ cancer cells, and myeloid cells in tumors. This results in blocking downstream signal transduction on cytotoxic T cells. It has been recently discovered that not only IFNγ but also HIF1α induces the expression of inhibitory molecule PD-L1 in tumor cells, and TAMs (9). Based on the literature, we hypothesized that ablation of "true" hypoxia may help diminish PD-L1 expression in TAMs, in turn, impairs their suppressive capacity. To assess this, we established 21-day YUMMER 1.7 tumors, and then harvested tumor infiltrating immune cells and stained for PD-L1 along with F4/80. We demonstrated herein that reduced hypoxia substantially diminishes PD-L1 expression in F4/80+ cells (**Figure 4.11 A and B**).

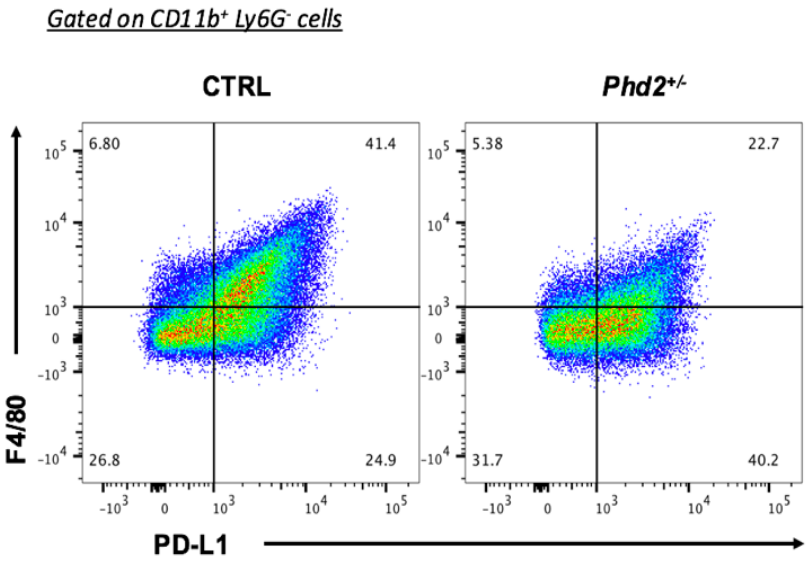

A.

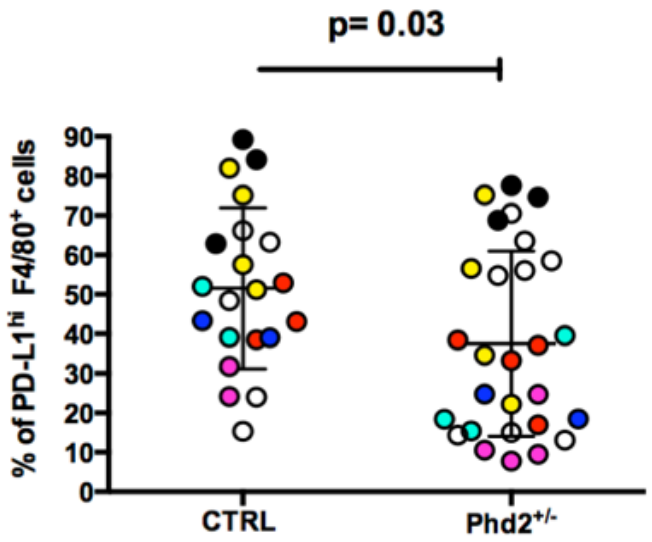

B.

Figure 4.11. Hypoxia reduction decreases the expression of PD-L1 on myeloid cells in melanoma tumors. Representative flow cytogram depicting PD-L1 expression in CD11b+ Ly6G- myeloid cells. Quantification of expression of PD-L1 in TAMs. Data are pooled from at least seven independent experiments. Each color represented independent experiments. Matched experiments are indicated by the same color.

5. DISCUSSION

Blood vessels in tumors are structurally and functionally aberrant (4). These structural aberrations result in hypoperfusion and hypoxia, which stimulate cancer cells to metastasize in different organs (36, 37). Under physiologic conditions, angiogenesis produces structurally intact and functioning blood vessels, thereby improving oxygenation (38). On the other hand, angiogenesis in the context of cancer is non-productive as the endothelial cell alignment is abnormal and blood vessels are blunted (39, 40). Consistent with *Mazzone et al*., we were able to demonstrate that blood vessels in PHD2 haplodeficient mice were significantly more elongated than WT mice (**Figure 4.1**). In addition, blood vessels in WT mice were blunted and fragile. In order to assess tumor vessel leakiness, which is a surrogate of vessel functionality, Texas-Red conjugated Dextran or FITC-conjugated lectin could be injected into mice (41, 42). Leaky and fragile vessel structure has been correlated with increased interstitial fluid pressure (IFP) in certain human cancers (eg, metastatic melanoma and breast cancer) (43-45). Instead of showing leakiness of tumor vessels, we stained tumor sections with fluorescence conjugated VE-Cadherin antibody to compare vessel maturation in $PHD2^{+/-}$ and WT mice (46). VE-Cadherin deficiency implicated in endothelial survival and adhesion (47, 48). Consistent with *Mazzone et al.*(5), PHD2 haplodeficient endothelial cells exhibit enhanced VE-Cadherin expression compared to WT (**Figure 4.2**). VE-Cadherin expression is regulated by HIF-2α via oxygen-independent mechanisms (49, 50). In addition, VEGF-VEGFR2 downstream signaling implicated in loosening of tight junctions between endothelial cells such as VE-Cadherin and ZO-1 (50, 51). Among many others, alpha smooth muscle actin (α-SMA) is a pericyte marker (52). Importantly, pericyte coverage of tumor vessels has been accepted as a prognostic factor in colorectal cancer (53). *Yonenaga et al.* investigated that vessel maturation is as important as vascular density. Beyond that, immature vascularization was associated with distant metastasis. Given this background, we stained tumor sections with fluorescence conjugated α-SMA and CD-146 antibodies to further our understanding of vascular maturity. Strikingly, we found that α-SMA and CD-146 staining merged in $PHD2^{+/-}$ endothelial cells obtained from YUMMER 1.7

tumor bearing mice but not in WT mice (**Figure 4.3**). Although there existed controversial knowledge pertaining to the implication of CD-146 expression on endothelial cells, this finding confirmed our initial hypothesis that PHD2 haplodeficiency enhanced endothelial cell integrity and maturation. In contrast to our finding, *Jiang et al.* highlighted that CD-146 plays a crucial role in angiogenesis in the context of tumor progression through binding to VEGFR-2 (54). However, growing body of literature demonstrated that CD-146 plays a key role in pericyte recruitment (55, 56). *Yan et al*. (57) recently highlighted that CD-146 binds to VEGF-C to control lymphangiogenesis. It has not been elucidated yet that whether $PHD2^{+/-}$ endothelial cells show lymphatic or blood vessel features in tumor microenvironment. Further studies are warranted to shed light on how $PHD2^{+/-}$ shapes the formation of conduits which may have an implication in lymphocyte infiltration. Given the misalignment of endothelial cells in the context of tumorigenesis, oxygen supply impaired. Vessel integrity and maturation is not only critical for adequate oxygen and nutrient supply to the tissues but also impacted extravasation of cancer cells and immune cells. It has been previously showed that improved endothelial cell alignment was associated with diminished tumor metastasis and enhanced drug delivery (58).

First anti-angiogenic therapy utilized by oncologists in 2004 upon receiving an approval by FDA for treatment-naive metastatic colorectal cancer in combination with chemotherapy (59). However, growing body of research suggested that anti-angiogenic treatments yielded a clinical benefit only for a limited window period which then was termed as normalization window (39, 60, 61). Blood vessel normalization typically begins within 1-2 days of starting anti-angiogenic treatment and lasts for 7-10 day. Beyond this window, VEGF blockades might increase tumor hypoxia, resulting in vessel sprouting (62). Above-mentioned studies have suggested that efficacy of anti-angiogenic treatments depended on scheduling and dosing that help normalize blood vessels rather than completely destroying angiogenesis (61). In parallel to this concept, *Zhou et al* (63) highlighted that lower than therapeutic dose of sunitinib in combination with temozolomide synergized to combat intractable brain tumors.

Anti-VEGF treatment may potentiate cancer immunotherapy by administering lower “vascular normalizing” doses of anti-angiogenic agents. PHD2 haplodeficiency normalized tumor blood vessels, thereby increasing PVC coverage and perfusion which lead to enhanced anti-tumor T cell infiltration. Together, these findings demonstrate that vessel normalization mediates improved immune cell infiltration and functionality. Lower “vascular normalizing” doses of anti-angiogenic treatment (10 or 20 mg/kg given every three days) redirect the TME from immunosuppressive to immunopermissive and potentiate the anti-cancer immunotherapy. Abnormal vasculature restrains anti-tumor T cell infiltration into tumor. In order to delineate the role of vascular normalization in T cell infiltration, extravasation experiment could be performed.

Hypoxia is a well-known aspect of solid tumors. It has been linked to poorer prognosis in majority of patients with solid tumors (64, 65). Although hypoxia has been extensively studied thus far by comparing the impact of 21% oxygen and 5-0.5% oxygen levels in vitro, tissue oxygenation in a living organism is far more complicated. Tissue oxygenation varies depending on the metabolic need and localization of the organ system. For instance, under normal circumstances, the epidermis of the skin has a partial oxygen pressure varying from 10% to 0.5% (66). It has been demonstrated that supplementary oxygenation of mice with aggressive form of lung cancer suggested that anti-tumor immune response was heightened when tumor hypoxia was disrupted (67). However, it remains to be determined how breathing 60% of oxygen influences tissue homeostasis throughout the body. Using a well-defined mouse model to reduce hypoxia and normalization of endothelial cell alignment, we were able to demonstrate that hypoxia reduction mounts anti-tumor immunity and slows tumor progression. Immune infiltration is one of the essential elements of desirable immunotherapy outcome. The Immunoscore developed by *Galon et al* (68) in 2006 proposed to classify tumors according to immune cell density (high vs low) and localization (tumor core vs margin) (69). Based on the immune infiltration, tumors are divided into 3 categories. These are immunologically cold, altered, and hot tumors (70). Immunologically cold tumor describes poor anti-tumor

immune infiltration. It has been linked to poor clinical outcome in vast majority of tumor types including melanoma (71, 72). Therefore, among many others, improving anti-tumor immune cell infiltration is one alternative approach to improve immunotherapy outcome which greatly varies between patients. Herein, we demonstrated that spatial distribution of tumor infiltrating immune cells is not homogenous.

In order to visualize CD4+ and CD8+ T cells along with in vivo hypoxia imaging, we utilized a well-established hypoxia probe (i.e hypoxyprobe) (73, 74). *Ragnum et al.* (75) exploited the same method to measure hypoxia levels of prostate cancers in humans. They were able to demonstrate that hypoxia levels of human prostate cancers were correlated with Gleason score, clinical stage, and lymph node metastasis. Participants of the study did not exhibit any adverse effects following to intravenous pimonidazole injection 20 minutes prior to the surgery. Increasing number of studies utilizing the methods such as pimonidazole staining, blood oxygen level-dependent imaging (BOLD-MRI) or PET with ^{18}F-labelled nitroimidazole would encourage clinicians to assess in situ oxygenation of tissues (75-77). Our research highlighted that hypoxic zones within tumors lack tumor-reactive CD8+ T cells (**Figure 4.4**). Although intrinsic effect of master transcription factor of hypoxia (HIF-1α) and hypoxic exclusion of CD8+ T cells remain controversial, our study showed that CD8+ and CD4+ T cells preferentially did not enter into poorly perfused tumor regions in accordance with the study led by *Hatfield et al.* (67). Nevertheless, some research groups showed that in vitro cultured CD8+ T cells under normoxic and hypoxic conditions exhibited similar distribution velocity into established B16 tumors (78). Their observation, however, also confirmed that both hypoxic or normoxic CD8+ T cells accumulated around perivascular tumor regions. It has been well established that in vitro hypoxia did not completely mimic in vivo hypoxia (20). Therefore, hypoxia researchers should vigilantly interrogate the results regarding the experimental settings (79). In other studies, researchers investigated that hyperoxic breathing (i.e 60% oxygen) reduced tumor burden and distant metastasis in an NK cell dependent manner. Intriguingly, they demonstrated that hyperoxia influenced

CD4+ and CD8+ T cell infiltration differentially. Although our imaging data regarding differential infiltration of CD4+ and CD8+ T cells in hypoxic regions in WT mice demonstrated a moderate difference between CD4+ and CD8+ T cells, enhanced CD8+ T cell infiltration in normoxic region was more robust than enhanced CD4+ T cell infiltration in PHD2 haplodeficient mice. Of note, FoxP3+ CD4+ T cells could make up a large proportion of hypoxic CD4+ T cells due to recruitment of Treg cells via hypoxia-induced CCL28 expression (80). Hence, further studies to elucidate what type of CD4 T cells are able to infiltrate in hypoxic zones of tumors are warranted. It would be a potential area of research that which cytokines and chemokines mediate improved CD8+ T cell infiltration in normoxic tumor regions. Prior studies demonstrated that CD8+ T cell recruitment was not solely dependent on chemokine and cytokine receptor-ligand interactions in the milieu. In fact, certain metabolites can contribute for the impediment to CD8+ T cell infiltration in hypoxic tumor regions (81, 82). For instance, oxygen shortage skews cellular metabolism towards glycolytic metabolism. Resultant accumulation of lactate may restrict T cell proliferation as shown in a prior study led by *Angelin et al* (83). Furthermore, *Angelin et al.* were able to demonstrate that lactate-rich environments induce FoxP3+ Treg differentiation. More importantly, this inhibitory effect of lactate on effector CD4+ T cell differentiation was reversed by lactate dehydrogenase inhibition. Contrary to this study, *Dang et al* demonstrated that HIF-1α controls cellular fate of Th17 and Treg cells. According to their study, HIF-1α skews Treg differentiation towards Th17 through degradation of FoxP3 protein and activation of RORγt (84). In a nutshell, further studies are warranted to delineate what factors mediate improved T cell infiltration within normoxic tumor regions. It could be chemokine, cytokine, and/or some other metabolites. In order to analyze metabolites, tumor interstitial fluid could be collected from harvested tumor tissues and be analyzed by mass spectrometry.

Having investigated that CD8+ T cells excluded from hypoxic tumor regions we sought to determine CD4+ and CD8+ T cell density in tumors with improved tissue oxygenation via PHD2 haplodeficiency. In consistent with the above-mentioned findings, we were able to demonstrate that vessel normalization and resultant

mitigation of tumor hypoxia in PHD2$^{+/-}$ mice significantly improved CD8+ T cell infiltration (**Figure 4.5**). However, CD4+ T cell infiltration increased to some extent due to a great variability of CD4+ T cell infiltration in WT mice. With keeping in mind this variation, our finding suggested that improved oxygenation via PHD2$^{+/-}$ preferentially promotes CD8+ T cell infiltration. Consistently, *Hatfield et al.* (67) drawn the conclusion that CD4+ and CD8+ T cells differentially affected by hypoxia.

After demonstrating enhanced T cell infiltration in PHD2 haplodeficient mice by imaging, we next monitored the tumor growth. Our study highlighted that, in parallel to improved T cell infiltration, tumor burden in PHD2$^{+/-}$ mice bearing YUMMER 1.7 melanoma tumors was significantly reduced (**Figure 4.6**). Not surprisingly, in vivo CD4 and CD8 T cell depletion abrogated this effect of PHD2$^{+/-}$. In conclusion, PHD2 haplodeficiency delayed tumor growth in a T cell dependent manner. Nevertheless, it has been previously investigated that PHD2$^{+/-}$ inhibits tumor metastasis but not tumor growth in LLC, B16, and Panc02 tumor models (5). These tumor models were best known for their poor immunogenicity which is determined by weak immunotherapy response (85, 86). Therefore, PHD2$^{+/-}$ mediated delayed tumor growth seems to be tumor model dependent. In addition to highly immunogenic YUMMER 1.7 melanoma model, subcutaneously injected mouse MC38 colon adenocarcinoma and B16-GP33 melanoma cells in WT and PHD2$^{+/-}$ mice confirmed delayed tumor growth by PHD2 haplodeficiency (not shown). We attributed the difference between tumor growth findings to highly immunogenic aspects of MC38, B16-GP33, and YUMMER 1.7 models (6, 28, 86-88). B16-GP33 cells express the LCMV glycoprotein peptide gp33. B16-GP33 cells are recognized by P14 TCR-Tg CD8+ T cells (89). We next sought to measure tumor infiltrating T cell density. Our measurement of T cell density, total T cell number divided by tumor weight, showed that both CD4 and CD8 T cell density was increased by PHD2 haplodeficiency (**Figure 4.7**). Our flow cytometric analysis and imaging data were consistent.

We then characterized CD8 T cell surface markers. To our surprise, we could not detect any difference pertaining to expression of exhaustion markers such as PD-1, Lag-3, CD38, and CD39 (**Figure 4.8**). It has been recently acknowledged that PD-1

expression was rapidly upregulated when naïve CD8 T cells were activated by lymphocytic choriomeningitis virus (LCMV) infection (90). CD39 expression on TILs has been correlated to chronic antigenic stimulation and bystander T cells (91). As opposed to tumor specific CD8+ T cells, bystander CD8+ T cells were not activated by tumor specific antigens. On the other hand, *Canale et al*. (92) demonstrated that CD39 is an exhaustion marker and could be targeted to potentiate immunotherapy response. Although there are controversial studies regarding hypoxia and T cell effector functions, *Doedens et al* (93) showed that Von Hippel Lindau (VHL) deficient CD8 T cells had elevated HIF-1a and, in turn, enhanced effector CD8+ T cell function. Therefore, bone marrow chimera experiment could shed light on this controversy by ruling out intrinsic effect of Phd2 haplodeficiency. However, sustained HIF-1α expression was also associated with increased PD-1, Lag-3, CTLA-4, and TIM-3 expression on CD8+ T cells. In accordance with this study, *Gropper et al* (78) highlighted that CD8+ T cells cultured under hypoxic conditions (eg, 1% oxygen) had more cytotoxic potential (eg, improved granzyme B and perforin production) than CTLs cultured under normoxic conditions (eg, 20% oxygen). *Clever et al.* (94) further confirmed that expression of PHD proteins promoted CTL tolerance and their inhibition enhanced anti-tumor immune response. They highlighted that PHD proteins compromise IFNg-mediated tumor regression. Although we cannot rule out intrinsic effect of PHD2 deficiency on CD8+ T cells, we initially hypothesized that reduced tumor burden in PHD2$^{+/-}$ mice could be related to reduced PD-1, Lag-3, CD38, or CD39 expression. However, it could be counterbalanced by increased HIF-1α expression on CD8 T cells due to PHD2 haplodeficiency.

After showing that true exhaustion state of CD8+ T cells in PHD2$^{+/-}$ and WT mice could not be determined by surface markers due to possible intrinsic effect of PHD2 haplodeficiency on CD8 T cells, we next analyzed IFNγ and TNF-α production. Contrary to surface markers, functional analysis of TILs (eg, IFNγ and TNF-α production) more accurately defined exhausted and less exhausted cells. As expected, less hypoxic CD8 T cells in PHD2$^{+/-}$ mice exhibited significantly improved IFNγ and TNF-α production (**Figure 4.9**) Interestingly, *Clever et al.* (94) showed that

PHD proteins (1-2-3) limited IFNγ production of CD4 and CD8 T cells, thereby contributing to respiratory tolerance. However, Treg frequency did not differ in CD4 $Cre^{+/-}$ $Egln1^{fl/fl}$ $Egln2^{fl/fl}$ $Egln3^{fl/fl}$ and WT mice. Even though this finding confirmed that triple PHD deficiency did not have an intrinsic effect on Treg induction, PHD deficiency of CD4+ T cells promoted IFNγ production of CD4+ and CD8+ T cells. Paracrine effect on CD8+ T cells could have been originated from diminished Th2 differentiation of CD4+ T cells due to triple PHD deficiency. Although *Clever et al.* knocked out all three isoforms of PHD proteins, we cannot exclude the possibility that PHD2 haplodeficiency on CD4+ and CD8+ T cells contributed to our findings. Further experiments should focus on ruling out of intrinsic effect of PHD2 deficiency.

Besides CD8 T cells, macrophages play a magnificent role in tumor clearance and tumor growth (10). Our study demonstrated that tumor-promoting macrophages (M2-like) preferentially infiltrated into poorly oxygenated tumor regions in agreement with prior investigations (**Figure 4.10**) (8, 95, 96). Therefore, disruption of hypoxia through blood vessel normalization diminishes M2-like macrophage frequency and, in turn, possibly improves the infiltration of tumor-reactive CD8+ T cell within tumors. It has been previously shown that hypoxia regulates macrophage phenotypes (95). M2-like macrophages retain in hypoxic tumor regions. Consequently, mitigation of hypoxia via $PHD2^{+/-}$ restricts M2-like macrophage infiltration within tumors. Beyond that, PD-L1 expression on $F4/80^{+}$ macrophages which indicates their suppression capacity was impaired in response to diminished hypoxia (**Figure 4.11**).

In conclusion, mitigation of hypoxia sculpts tumor microenvironment through improved CD4+ and CD8+ T cell infiltration, greater TNF-α and IFN-γ production, and impaired M2-like macrophage infiltration. However, we could not detect differential expression of exhaustion markers (eg, PD-1, Lag-3, CD38, and CD39). We speculated that these markers would be upregulated upon T cell activation, in turn, do not necessarily show “true” exhaustion. Further investigation will explore whether or not improved T cell influx occurs due to diminished M2-like macrophage infiltration. On the other hand, extravasation of T cells depends on the expression of selectins and

integrins on endothelial cells, which needs to be further dissected. Single cell RNA sequencing should be performed to gain an insight what genes of TILs are regulated by normalized tumor vasculature and resultant diminished hypoxia. A previous study demonstrated that hypoxia genes of melanoma patients who are irresponsive to anti-PD1 therapy were enriched. These findings support of hypoxia mitigation helps improve anti-tumor immune response. Therefore, clinical trials are warranted to confirm our promising data.

6. CONCLUSIONS AND REMARKS

1. PHD2 haplodeficiency helps normalize endothelial cell alignment. PHD2 haplodeficient blood vessels are more elongated than WT. Moreover, integrity of blood vessels in $PHD2^{+/-}$ mice is enhanced.
2. CD4 and CD8 T cells in melanoma TME preferentially infiltrate in normoxic tumor regions.
3. Mitigation of hypoxia via $PHD2^{+/-}$ improves CD4 and CD8 T cell density in melanoma tumors.
4. Expression of PD-1, Lag-3, CD38, and CD39 are not changed with improved oxygenation.
5. IFNg production of CD8 T cells is significantly improved in $PHD2^{+/-}$ mice.
6. Pro-inflammatory macrophage infiltration strikingly enhanced by $PHD2^{+/-}$ haplodeficiency.
7. Pro-tumorigenic M2-like macrophages make a large proportion of tumor infiltrating macrophages and $PHD2^{+/-}$ slightly mitigate $F4/80^{+}$ M2-like macrophage infiltration.
8. Although there is a slight decrease in the percentage of M2-like macrophages, PD-L1 expression on M2-like macrophages is significantly diminished by $PHD2^{+/-}$.
9. Single cell RNA sequencing should be performed to gain an insight what genes of TILs are regulated by normalized tumor vasculature and resultant diminished hypoxia.
10. Further studies are warranted to delineate what factors mediate improved T cell infiltration within normoxic tumor regions.

7. REFERENCES

1. Flaherty KT, Infante JR, Daud A, Gonzalez R, Kefford RF, Sosman J, et al. Combined BRAF and MEK inhibition in melanoma with BRAF V600 mutations. N Engl J Med. 2012;367(18):1694-703.
2. Spranger S, Spaapen RM, Zha Y, Williams J, Meng Y, Ha TT, et al. Up-regulation of PD-L1, IDO, and T(regs) in the melanoma tumor microenvironment is driven by CD8(+) T cells. Sci Transl Med. 2013;5(200):200ra116.
3. Herbst RS, Soria JC, Kowanetz M, Fine GD, Hamid O, Gordon MS, et al. Predictive correlates of response to the anti-PD-L1 antibody MPDL3280A in cancer patients. Nature. 2014;515(7528):563-7.
4. Schaaf MB, Garg AD, Agostinis P. Defining the role of the tumor vasculature in antitumor immunity and immunotherapy. Cell Death Dis. 2018;9(2):115.
5. Mazzone M, Dettori D, de Oliveira RL, Loges S, Schmidt T, Jonckx B, et al. Heterozygous deficiency of PHD2 restores tumor oxygenation and inhibits metastasis via endothelial normalization. Cell. 2009;136(5):839-51.
6. Lane RS, Femel J, Breazeale AP, Loo CP, Thibault G, Kaempf A, et al. IFNγ-activated dermal lymphatic vessels inhibit cytotoxic T cells in melanoma and inflamed skin. J Exp Med. 2018;215(12):3057-74.
7. Hamzah J, Jugold M, Kiessling F, Rigby P, Manzur M, Marti HH, et al. Vascular normalization in Rgs5-deficient tumours promotes immune destruction. Nature. 2008;453(7193):410-4.
8. Casazza A, Laoui D, Wenes M, Rizzolio S, Bassani N, Mambretti M, et al. Impeding macrophage entry into hypoxic tumor areas by Sema3A/Nrp1 signaling blockade inhibits angiogenesis and restores antitumor immunity. Cancer Cell. 2013;24(6):695-709.
9. Noman MZ, Desantis G, Janji B, Hasmim M, Karray S, Dessen P, et al. PD-L1 is a novel direct target of HIF-1α, and its blockade under hypoxia enhanced MDSC-mediated T cell activation. J Exp Med. 2014;211(5):781-90.
10. Perry CJ, Muñoz-Rojas AR, Meeth KM, Kellman LN, Amezquita RA, Thakral D, et al. Myeloid-targeted immunotherapies act in synergy to induce inflammation and antitumor immunity. J Exp Med. 2018;215(3):877-93.
11. Siegel RL, Miller KD, Jemal A. Cancer statistics, 2020. CA Cancer J Clin. 2020;70(1):7-30.
12. Saito M, Momma T, Kono K. Targeted therapy according to next generation sequencing-based panel sequencing. Fukushima J Med Sci. 2018;64(1):9-14.
13. Chapman PB, Hauschild A, Robert C, Haanen JB, Ascierto P, Larkin J, et al. Improved survival with vemurafenib in melanoma with BRAF V600E mutation. N Engl J Med. 2011;364(26):2507-16.

14. Hauschild A, Grob JJ, Demidov LV, Jouary T, Gutzmer R, Millward M, et al. Dabrafenib in BRAF-mutated metastatic melanoma: a multicentre, open-label, phase 3 randomised controlled trial. Lancet. 2012;380(9839):358-65.

15. Saei A, Eichhorn PJA. Adaptive Responses as Mechanisms of Resistance to BRAF Inhibitors in Melanoma. Cancers (Basel). 2019;11(8).

16. Hazarika M, Chuk MK, Theoret MR, Mushti S, He K, Weis SL, et al. U.S. FDA Approval Summary: Nivolumab for Treatment of Unresectable or Metastatic Melanoma Following Progression on Ipilimumab. Clin Cancer Res. 2017;23(14):3484-8.

17. Falcone I, Conciatori F, Bazzichetto C, Ferretti G, Cognetti F, Ciuffreda L, et al. Tumor Microenvironment: Implications in Melanoma Resistance to Targeted Therapy and Immunotherapy. Cancers (Basel). 2020;12(10).

18. Gray LH, Conger AD, Ebert M, Hornsey S, Scott OC. The concentration of oxygen dissolved in tissues at the time of irradiation as a factor in radiotherapy. Br J Radiol. 1953;26(312):638-48.

19. Rockwell S, Dobrucki IT, Kim EY, Marrison ST, Vu VT. Hypoxia and radiation therapy: past history, ongoing research, and future promise. Curr Mol Med. 2009;9(4):442-58.

20. Carreau A, El Hafny-Rahbi B, Matejuk A, Grillon C, Kieda C. Why is the partial oxygen pressure of human tissues a crucial parameter? Small molecules and hypoxia. J Cell Mol Med. 2011;15(6):1239-53.

21. Wilson GK, Tennant DA, McKeating JA. Hypoxia inducible factors in liver disease and hepatocellular carcinoma: current understanding and future directions. J Hepatol. 2014;61(6):1397-406.

22. Semenza GL. HIF-1, O(2), and the 3 PHDs: how animal cells signal hypoxia to the nucleus. Cell. 2001;107(1):1-3.

23. Kaelin WG, Jr. The VHL Tumor Suppressor Gene: Insights into Oxygen Sensing and Cancer. Trans Am Clin Climatol Assoc. 2017;128:298-307.

24. Wang GL, Jiang BH, Rue EA, Semenza GL. Hypoxia-inducible factor 1 is a basic-helix-loop-helix-PAS heterodimer regulated by cellular O2 tension. Proc Natl Acad Sci U S A. 1995;92(12):5510-4.

25. Kaelin WG, Jr., Ratcliffe PJ. Oxygen sensing by metazoans: the central role of the HIF hydroxylase pathway. Mol Cell. 2008;30(4):393-402.

26. Tao JH, Barbi J, Pan F. Hypoxia-inducible factors in T lymphocyte differentiation and function. A Review in the Theme: Cellular Responses to Hypoxia. Am J Physiol Cell Physiol. 2015;309(9):C580-9.

27. Jain RK. Antiangiogenesis strategies revisited: from starving tumors to alleviating hypoxia. Cancer Cell. 2014;26(5):605-22.

28. Wang J, Perry CJ, Meeth K, Thakral D, Damsky W, Micevic G, et al. UV-induced somatic mutations elicit a functional T cell response in the YUMMER1.7 mouse melanoma model. Pigment Cell Melanoma Res. 2017;30(4):428-35.

29. Fischer K, Hoffmann P, Voelkl S, Meidenbauer N, Ammer J, Edinger M, et al. Inhibitory effect of tumor cell-derived lactic acid on human T cells. Blood. 2007;109(9):3812-9.

30. Bardin N, Anfosso F, Massé JM, Cramer E, Sabatier F, Le Bivic A, et al. Identification of CD146 as a component of the endothelial junction involved in the control of cell-cell cohesion. Blood. 2001;98(13):3677-84.

31. Ho PC, Bihuniak JD, Macintyre AN, Staron M, Liu X, Amezquita R, et al. Phosphoenolpyruvate Is a Metabolic Checkpoint of Anti-tumor T Cell Responses. Cell. 2015;162(6):1217-28.

32. Scharping NE, Menk AV, Moreci RS, Whetstone RD, Dadey RE, Watkins SC, et al. The Tumor Microenvironment Represses T Cell Mitochondrial Biogenesis to Drive Intratumoral T Cell Metabolic Insufficiency and Dysfunction. Immunity. 2016;45(2):374-88.

33. Philip M, Fairchild L, Sun L, Horste EL, Camara S, Shakiba M, et al. Chromatin states define tumour-specific T cell dysfunction and reprogramming. Nature. 2017;545(7655):452-6.

34. Huang AC, Postow MA, Orlowski RJ, Mick R, Bengsch B, Manne S, et al. T-cell invigoration to tumour burden ratio associated with anti-PD-1 response. Nature. 2017;545(7652):60-5.

35. Veglia F, Perego M, Gabrilovich D. Myeloid-derived suppressor cells coming of age. Nat Immunol. 2018;19(2):108-19.

36. Sullivan R, Graham CH. Hypoxia-driven selection of the metastatic phenotype. Cancer Metastasis Rev. 2007;26(2):319-31.

37. Rankin EB, Giaccia AJ. Hypoxic control of metastasis. Science. 2016;352(6282):175-80.

38. Papetti M, Herman IM. Mechanisms of normal and tumor-derived angiogenesis. Am J Physiol Cell Physiol. 2002;282(5):C947-70.

39. Jain RK. Normalization of tumor vasculature: an emerging concept in antiangiogenic therapy. Science. 2005;307(5706):58-62.

40. Forster JC, Harriss-Phillips WM, Douglass MJ, Bezak E. A review of the development of tumor vasculature and its effects on the tumor microenvironment. Hypoxia (Auckl). 2017;5:21-32.

41. Hashizume H, Baluk P, Morikawa S, McLean JW, Thurston G, Roberge S, et al. Openings between defective endothelial cells explain tumor vessel leakiness. Am J Pathol. 2000;156(4):1363-80.

42. Honkura N, Richards M, Laviña B, Sáinz-Jaspeado M, Betsholtz C, Claesson-Welsh L. Intravital imaging-based analysis tools for vessel identification and assessment of concurrent dynamic vascular events. Nat Commun. 2018;9(1):2746.

43. Stylianopoulos T, Munn LL, Jain RK. Reengineering the Physical Microenvironment of Tumors to Improve Drug Delivery and Efficacy: From Mathematical Modeling to Bench to Bedside. Trends Cancer. 2018;4(4):292-319.

44. Heldin CH, Rubin K, Pietras K, Ostman A. High interstitial fluid pressure - an obstacle in cancer therapy. Nat Rev Cancer. 2004;4(10):806-13.

45. Boucher Y, Jain RK. Microvascular pressure is the principal driving force for interstitial hypertension in solid tumors: implications for vascular collapse. Cancer Res. 1992;52(18):5110-4.

46. Duong CN, Vestweber D. Mechanisms Ensuring Endothelial Junction Integrity Beyond VE-Cadherin. Front Physiol. 2020;11:519.

47. Carmeliet P, Lampugnani MG, Moons L, Breviario F, Compernolle V, Bono F, et al. Targeted deficiency or cytosolic truncation of the VE-cadherin gene in mice impairs VEGF-mediated endothelial survival and angiogenesis. Cell. 1999;98(2):147-57.

48. Lagendijk AK, Hogan BM. VE-cadherin in vascular development: a coordinator of cell signaling and tissue morphogenesis. Curr Top Dev Biol. 2015;112:325-52.

49. Le Bras A, Lionneton F, Mattot V, Lelièvre E, Caetano B, Spruyt N, et al. HIF-2alpha specifically activates the VE-cadherin promoter independently of hypoxia and in synergy with Ets-1 through two essential ETS-binding sites. Oncogene. 2007;26(53):7480-9.

50. Gong H, Rehman J, Tang H, Wary K, Mittal M, Chaturvedi P, et al. HIF2α signaling inhibits adherens junctional disruption in acute lung injury. J Clin Invest. 2015;125(2):652-64.

51. Dejana E, Tournier-Lasserve E, Weinstein BM. The control of vascular integrity by endothelial cell junctions: molecular basis and pathological implications. Dev Cell. 2009;16(2):209-21.

52. Morikawa S, Baluk P, Kaidoh T, Haskell A, Jain RK, McDonald DM. Abnormalities in pericytes on blood vessels and endothelial sprouts in tumors. Am J Pathol. 2002;160(3):985-1000.

53. Yonenaga Y, Mori A, Onodera H, Yasuda S, Oe H, Fujimoto A, et al. Absence of smooth muscle actin-positive pericyte coverage of tumor vessels correlates with hematogenous metastasis and prognosis of colorectal cancer patients. Oncology. 2005;69(2):159-66.

54. Jiang T, Zhuang J, Duan H, Luo Y, Zeng Q, Fan K, et al. CD146 is a coreceptor for VEGFR-2 in tumor angiogenesis. Blood. 2012;120(11):2330-9.

55. Yamazaki T, Mukouyama YS. Tissue Specific Origin, Development, and Pathological Perspectives of Pericytes. Front Cardiovasc Med. 2018;5:78.

56. Chen J, Luo Y, Huang H, Wu S, Feng J, Zhang J, et al. CD146 is essential for PDGFRβ-induced pericyte recruitment. Protein Cell. 2018;9(8):743-7.

57. Yan H, Zhang C, Wang Z, Tu T, Duan H, Luo Y, et al. CD146 is required for VEGF-C-induced lymphatic sprouting during lymphangiogenesis. Sci Rep. 2017;7(1):7442.

58. Leite de Oliveira R, Deschoemaeker S, Henze AT, Debackere K, Finisguerra V, Takeda Y, et al. Gene-targeting of Phd2 improves tumor response to chemotherapy and prevents side-toxicity. Cancer Cell. 2012;22(2):263-77.

59. Hurwitz H, Fehrenbacher L, Novotny W, Cartwright T, Hainsworth J, Heim W, et al. Bevacizumab plus irinotecan, fluorouracil, and leucovorin for metastatic colorectal cancer. N Engl J Med. 2004;350(23):2335-42.

60. Batchelor TT, Sorensen AG, di Tomaso E, Zhang WT, Duda DG, Cohen KS, et al. AZD2171, a pan-VEGF receptor tyrosine kinase inhibitor, normalizes tumor vasculature and alleviates edema in glioblastoma patients. Cancer Cell. 2007;11(1):83-95.

61. Winkler F, Kozin SV, Tong RT, Chae SS, Booth MF, Garkavtsev I, et al. Kinetics of vascular normalization by VEGFR2 blockade governs brain tumor response to radiation: role of oxygenation, angiopoietin-1, and matrix metalloproteinases. Cancer Cell. 2004;6(6):553-63.

62. Loges S, Mazzone M, Hohensinner P, Carmeliet P. Silencing or fueling metastasis with VEGF inhibitors: antiangiogenesis revisited. Cancer Cell. 2009;15(3):167-70.

63. Zhou Q, Gallo JM. Differential effect of sunitinib on the distribution of temozolomide in an orthotopic glioma model. Neuro Oncol. 2009;11(3):301-10.

64. Bertout JA, Patel SA, Simon MC. The impact of O2 availability on human cancer. Nat Rev Cancer. 2008;8(12):967-75.

65. Wilson WR, Hay MP. Targeting hypoxia in cancer therapy. Nat Rev Cancer. 2011;11(6):393-410.

66. Evans SM, Schrlau AE, Chalian AA, Zhang P, Koch CJ. Oxygen levels in normal and previously irradiated human skin as assessed by EF5 binding. J Invest Dermatol. 2006;126(12):2596-606.

67. Hatfield SM, Kjaergaard J, Lukashev D, Schreiber TH, Belikoff B, Abbott R, et al. Immunological mechanisms of the antitumor effects of supplemental oxygenation. Sci Transl Med. 2015;7(277):277ra30.

68. Galon J, Costes A, Sanchez-Cabo F, Kirilovsky A, Mlecnik B, Lagorce-Pages C, et al. Type, density, and location of immune cells within human colorectal tumors predict clinical outcome. Science. 2006;313(5795):1960-4.

69. Galon J, Costes A, Sanchez-Cabo F, Kirilovsky A, Mlecnik B, Lagorce-Pagès C, et al. Type, density, and location of immune cells within human colorectal tumors predict clinical outcome. Science. 2006;313(5795):1960-4.

70. Galon J, Bruni D. Approaches to treat immune hot, altered and cold tumours with combination immunotherapies. Nat Rev Drug Discov. 2019;18(3):197-218.

71. Fridman WH, Pagès F, Sautès-Fridman C, Galon J. The immune contexture in human tumours: impact on clinical outcome. Nat Rev Cancer. 2012;12(4):298-306.

72. Tumeh PC, Harview CL, Yearley JH, Shintaku IP, Taylor EJ, Robert L, et al. PD-1 blockade induces responses by inhibiting adaptive immune resistance. Nature. 2014;515(7528):568-71.

73. Scharping NE, Rivadeneira DB, Menk AV, Vignali PDA, Ford BR, Rittenhouse NL, et al. Mitochondrial stress induced by continuous stimulation under hypoxia rapidly drives T cell exhaustion. Nat Immunol. 2021.

74. Jayaprakash P, Ai M, Liu A, Budhani P, Bartkowiak T, Sheng J, et al. Targeted hypoxia reduction restores T cell infiltration and sensitizes prostate cancer to immunotherapy. J Clin Invest. 2018;128(11):5137-49.

75. Ragnum HB, Vlatkovic L, Lie AK, Axcrona K, Julin CH, Frikstad KM, et al. The tumour hypoxia marker pimonidazole reflects a transcriptional programme associated with aggressive prostate cancer. Br J Cancer. 2015;112(2):382-90.

76. Liang J, Cheng Q, Huang J, Ma M, Zhang D, Lei X, et al. Monitoring tumour microenvironment changes during anti-angiogenesis therapy using functional MRI. Angiogenesis. 2019;22(3):457-70.

77. O'Connor JPB, Robinson SP, Waterton JC. Imaging tumour hypoxia with oxygen-enhanced MRI and BOLD MRI. Br J Radiol. 2019;92(1095):20180642.

78. Gropper Y, Feferman T, Shalit T, Salame TM, Porat Z, Shakhar G. Culturing CTLs under Hypoxic Conditions Enhances Their Cytolysis and Improves Their Anti-tumor Function. Cell Rep. 2017;20(11):2547-55.

79. Caldwell CC, Kojima H, Lukashev D, Armstrong J, Farber M, Apasov SG, et al. Differential effects of physiologically relevant hypoxic conditions on T lymphocyte development and effector functions. J Immunol. 2001;167(11):6140-9.

80. Facciabene A, Peng X, Hagemann IS, Balint K, Barchetti A, Wang LP, et al. Tumour hypoxia promotes tolerance and angiogenesis via CCL28 and T(reg) cells. Nature. 2011;475(7355):226-30.

81. Buck MD, Sowell RT, Kaech SM, Pearce EL. Metabolic Instruction of Immunity. Cell. 2017;169(4):570-86.

82. Haas R, Smith J, Rocher-Ros V, Nadkarni S, Montero-Melendez T, D'Acquisto F, et al. Lactate Regulates Metabolic and Pro-inflammatory Circuits in Control of T Cell Migration and Effector Functions. PLoS Biol. 2015;13(7):e1002202.

83. Angelin A, Gil-de-Gómez L, Dahiya S, Jiao J, Guo L, Levine MH, et al. Foxp3 Reprograms T Cell Metabolism to Function in Low-Glucose, High-Lactate Environments. Cell Metab. 2017;25(6):1282-93.e7.

84. Dang EV, Barbi J, Yang HY, Jinasena D, Yu H, Zheng Y, et al. Control of T(H)17/T(reg) balance by hypoxia-inducible factor 1. Cell. 2011;146(5):772-84.

85. Lechner MG, Karimi SS, Barry-Holson K, Angell TE, Murphy KA, Church CH, et al. Immunogenicity of murine solid tumor models as a defining feature of in vivo behavior and response to immunotherapy. J Immunother. 2013;36(9):477-89.

86. He M, Henderson M, Muth S, Murphy A, Zheng L. Preclinical mouse models for immunotherapeutic and non-immunotherapeutic drug development for pancreatic ductal adenocarcinoma. Ann Pancreat Cancer. 2020;3.

87. Harjes U. Helping tumour antigens to the surface. Nat Rev Cancer. 2019;19(11):608.

88. Harel M, Ortenberg R, Varanasi SK, Mangalhara KC, Mardamshina M, Markovits E, et al. Proteomics of Melanoma Response to Immunotherapy Reveals Mitochondrial Dependence. Cell. 2019;179(1):236-50.e18.

89. Liu C, Peng W, Xu C, Lou Y, Zhang M, Wargo JA, et al. BRAF inhibition increases tumor infiltration by T cells and enhances the antitumor activity of adoptive immunotherapy in mice. Clin Cancer Res. 2013;19(2):393-403.

90. Ahn E, Araki K, Hashimoto M, Li W, Riley JL, Cheung J, et al. Role of PD-1 during effector CD8 T cell differentiation. Proc Natl Acad Sci U S A. 2018;115(18):4749-54.

91. Simoni Y, Becht E, Fehlings M, Loh CY, Koo SL, Teng KWW, et al. Bystander CD8(+) T cells are abundant and phenotypically distinct in human tumour infiltrates. Nature. 2018;557(7706):575-9.

92. Canale FP, Ramello MC, Núñez N, Araujo Furlan CL, Bossio SN, Gorosito Serrán M, et al. CD39 Expression Defines Cell Exhaustion in Tumor-Infiltrating CD8(+) T Cells. Cancer Res. 2018;78(1):115-28.

93. Doedens AL, Phan AT, Stradner MH, Fujimoto JK, Nguyen JV, Yang E, et al. Hypoxia-inducible factors enhance the effector responses of CD8(+) T cells to persistent antigen. Nat Immunol. 2013;14(11):1173-82.

94. Clever D, Roychoudhuri R, Constantinides MG, Askenase MH, Sukumar M, Klebanoff CA, et al. Oxygen Sensing by T Cells Establishes an Immunologically Tolerant Metastatic Niche. Cell. 2016;166(5):1117-31.e14.

95. Henze AT, Mazzone M. The impact of hypoxia on tumor-associated macrophages. J Clin Invest. 2016;126(10):3672-9.

96. Peterson TE, Kirkpatrick ND, Huang Y, Farrar CT, Marijt KA, Kloepper J, et al. Dual inhibition of Ang-2 and VEGF receptors normalizes tumor vasculature and prolongs survival in glioblastoma by altering macrophages. Proc Natl Acad Sci U S A. 2016;113(16):4470-5.

8. APPENDICES

APPENDIX-1: Ethical approval for Thesis Studies

Institutional Animal Care and Use Committee
(IACUC)

Salk Institute for Biological Studies
10010 N Torrey Pines Rd
La Jolla, California 92037
PH (858) 453-4100 x1591
FX (858) 824-1962
www.salk.edu

TO: Susan Kaech

FROM: Institutional Animal Care and Use Committee (IACUC)

DATE: Mar 16, 2018

SUBJECT: **ADMINISTRATIVE AMENDMENT APPROVAL**
Protocol Number: 17-00032
Protocol Title: Mechansims of T cell function during viral and bacterial infection and in cancer

Species Information: Mice
Approval Period: Feb 07, 2018 - Feb 07, 2021

Protocol Funding: (Funding Agency, Fund Title, Grant Number)

Added: NIH, CA216101

Note: To delete funding, please send an email request to iacucadmin@salk.edu.

Personnel Changes:

Personnel Added
Added: Victoria Tripple, Dan Chen, Ruveyda Ayasun

Note: To delete personnel, please send an email request to iacucadmin@salk.edu.

Your Animal Use **Protocol Amendmen**t requesting change of funding or personnel has been reviewed and approved administratively by the IACUC office staff.

The Grants Administration Office will be responsible for providing the documentation of IACUC approval to the funding agency.

cc: Grants Administration

APPENDIX-2: Thesis Originality Report

TO EXAMINE THE ROLE OF HYPOXIA ON ANTI-TUMOUR IMMUNITY

ORİJİNALLİK RAPORU

%20	%15	%15	%3
BENZERLİK ENDEKSİ	İNTERNET KAYNAKLARI	YAYINLAR	ÖĞRENCİ ÖDEVLERİ

BİRİNCİL KAYNAKLAR

1	rupress.org İnternet Kaynağı	%2
2	openaccess.hacettepe.edu.tr:8080 İnternet Kaynağı	%1
3	jitc.biomedcentral.com İnternet Kaynağı	%1
4	link.springer.com İnternet Kaynağı	%1
5	www.openaccess.hacettepe.edu.tr:8080 İnternet Kaynağı	%1
6	repository.bilkent.edu.tr İnternet Kaynağı	%1
7	elischolar.library.yale.edu İnternet Kaynağı	<%1
8	www.frontiersin.org İnternet Kaynağı	<%1
9	Jake Wang, Curtis J. Perry, Katrina Meeth, Durga Thakral et al. "UV-induced somatic	<%1

APPENDIX-3: Digital Receipt

turnitin

Dijital Makbuz

Bu makbuz ödevinizin Turnitin'e ulaştığını bildirmektedir. Gönderiminize dair bilgiler şöyledir:

Gönderinizin ilk sayfası aşağıda gönderilmektedir.

Gönderen:	Ruveyda Ayasun
Ödev başlığı:	Ruveyda Tez
Gönderi Başlığı:	TO EXAMINE THE ROLE OF HYPOXIA ON ANTI-TUMOUR IMM...
Dosya adı:	To_Examine_the_Role_of_Hypoxia_on_Anti-tumour_Immunity....
Dosya boyutu:	47.63M
Sayfa sayısı:	99
Kelime sayısı:	13,692
Karakter sayısı:	79,678
Gönderim Tarihi:	04-May-2021 10:53PM (UTC+0300)
Gönderim Numarası:	1578048067